2009 fall

Advanced Physical Metallurgy

"Phase Equilibria in Materials"

10. 27. 2009

Eun Soo Park

Office: 33-316
Telephone: 880-7221
Email: espark@snu.ac.kr
Office hours: by an appointment

Contents for previous class

“Alloy solidification”

- Solidification of single-phase alloys

- **Three limiting cases**

1) Equilibrium Solidification: perfect mixing in solid and liquid

2) No Diffusion in Solid, Perfect Mixing in Liquid

3) No Diffusion on Solid, Diffusional Mixing in the Liquid

Planar S/L interface
→ unidirectional solidification

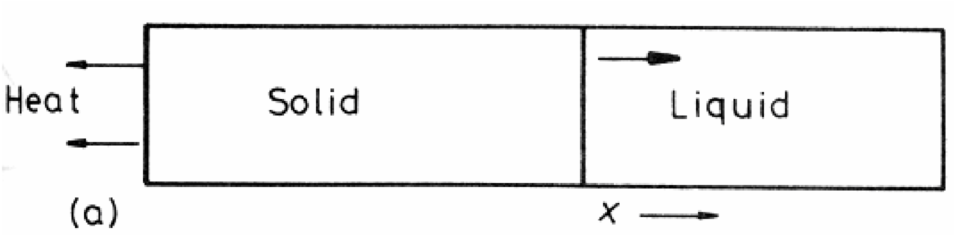

1) Equilibrium Solidification Low cooling rate

$$k = \frac{X_S}{X_L} < 1$$

k : partition coefficient

X : mole fraction of solute

In this phase diagram of straight solidus and liquidus, k is independent of T.

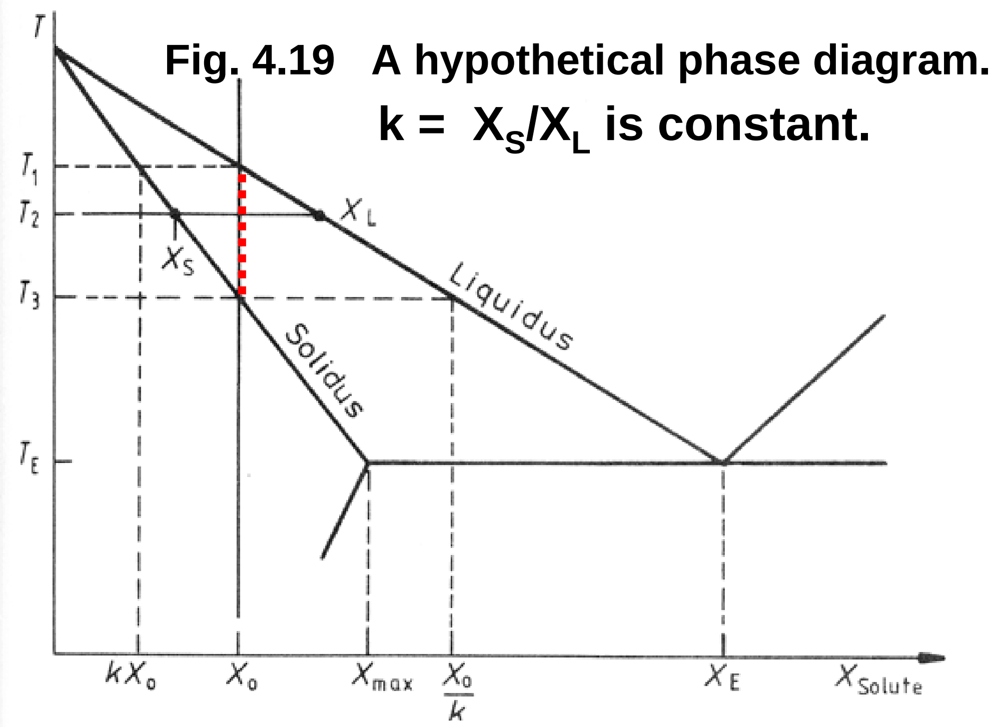

Fig. 4.19 A hypothetical phase diagram.

$k = X_S/X_L$ is constant.

- **Sufficient time for diffusion in solid & liquid**
- **Relative amount of solid and liquid : lever rule**
- **Solidification starts at T_1 ($X_s=kX_0$) and**

  ends at T_3 ($X_L=X_0/k$).

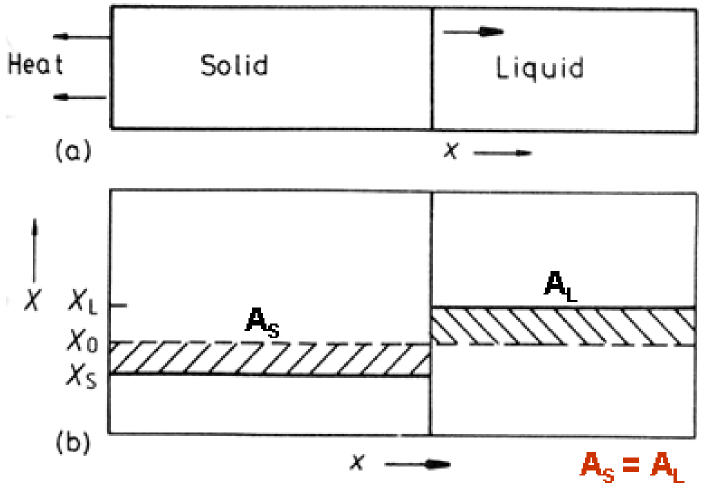

2) No Diffusion in Solid, Perfect Mixing in Liquid

: high cooling rate, efficient stirring

- Separate layers of solid retain their original compositions

  mean comp. of the solid ($\overline{X}_S$) < X_s
- Liquid become richer than $X_0/K \rightarrow X_E$
- Variation of X_s: solute rejected to the liquid

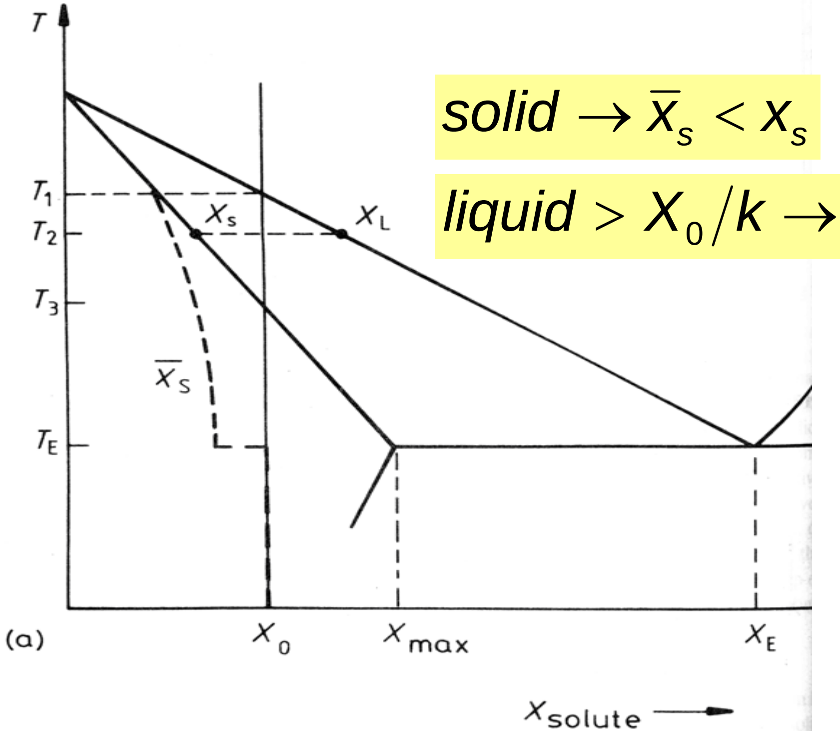

$solid \rightarrow \bar{x}_s < x_s$

$liquid > X_0/k \rightarrow X_E$

local equil. at S/L interface

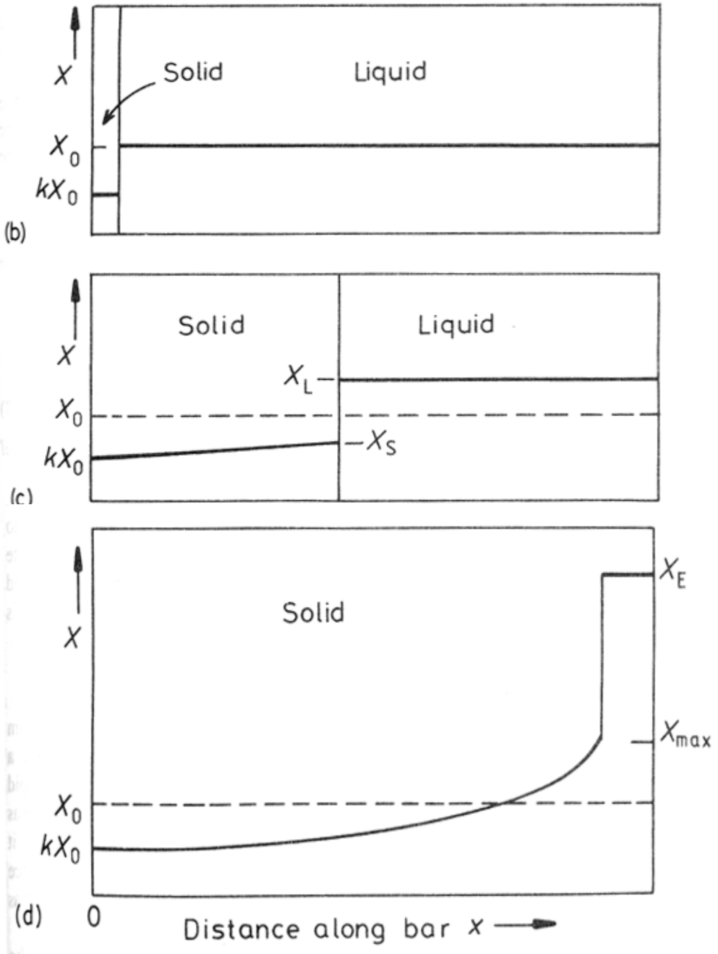

Fig. 4.21 Planar front solidification of alloy X_0 in fig. 4.19 assuming no diffusion in the solid, but complete mixing in the liquid. (a) As Fig. 4.19, but including the mean composition of the solid. (b) Composition profile just under T_1. (c) Composition profile at T_2 (compare with the profile and fraction solidified in Fig.4.20b) (d) Composition profile at the eutectic temperature and below.

3) No Diffusion on Solid, Diffusional Mixing in the Liquid

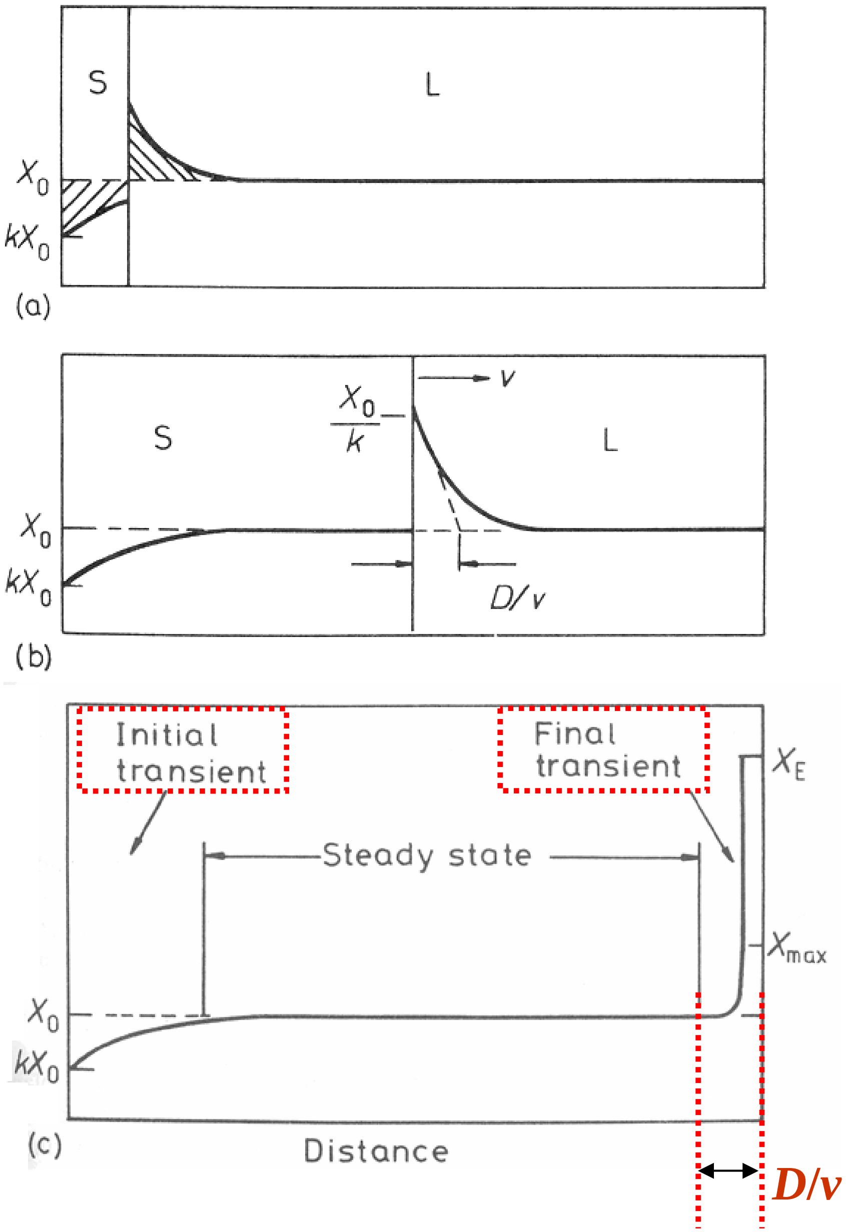

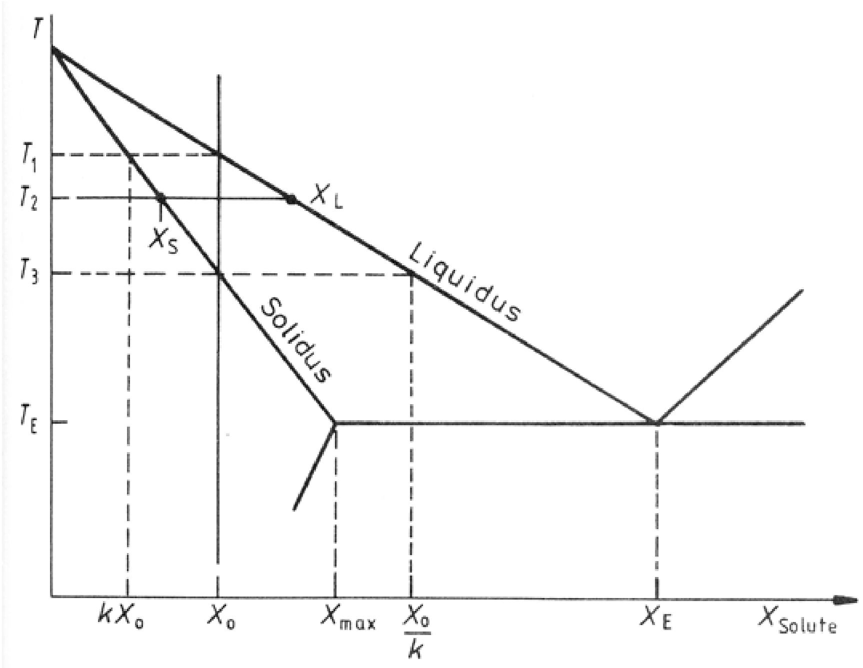

Fig. 4.22 Planar front solidification of alloy X_0 in Fig. 4.19 assuming no diffusion in solid and no stirring in the liquid.

(a) Composition profile when S/L temperature is between T_2 and T_3 in Fig. 4.19.

(b) Steady-state at T_3. The composition solidifying equals the composition of liquid far ahead of the solid (X_0).

(c) Composition profile at T_E and below, showing the final transient.

실제의 농도분포

두 가지 경우의 중간형태

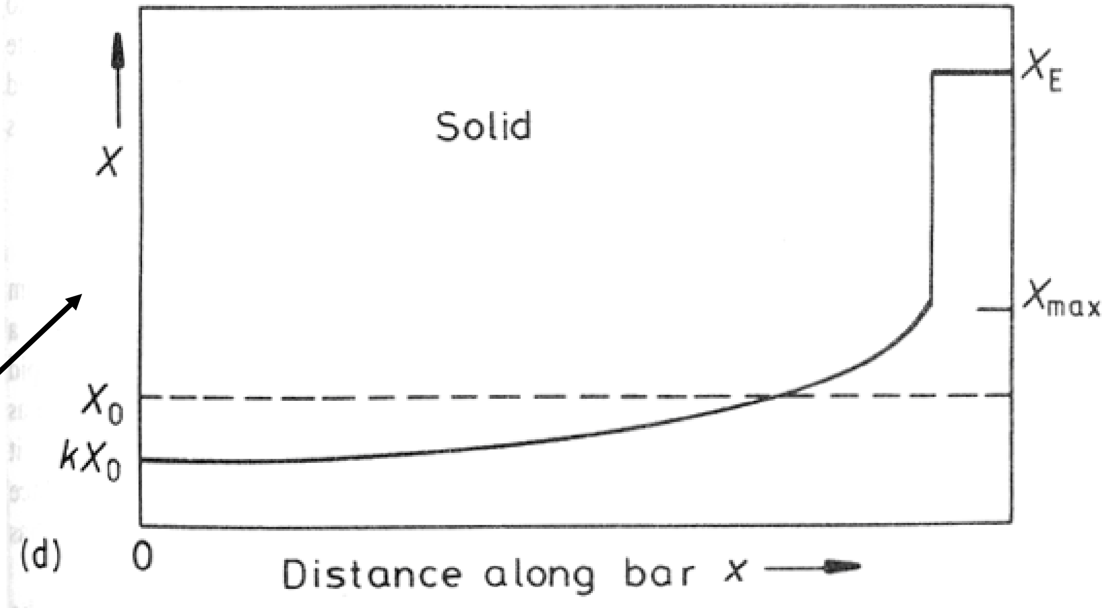

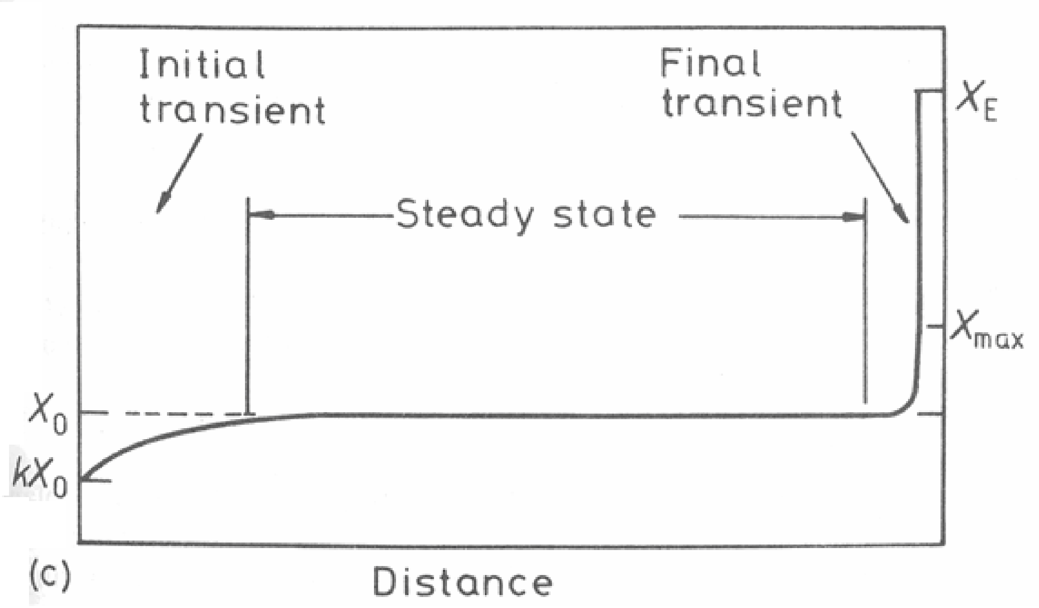

➡ **Zone Refining**

Constitutional Supercooling

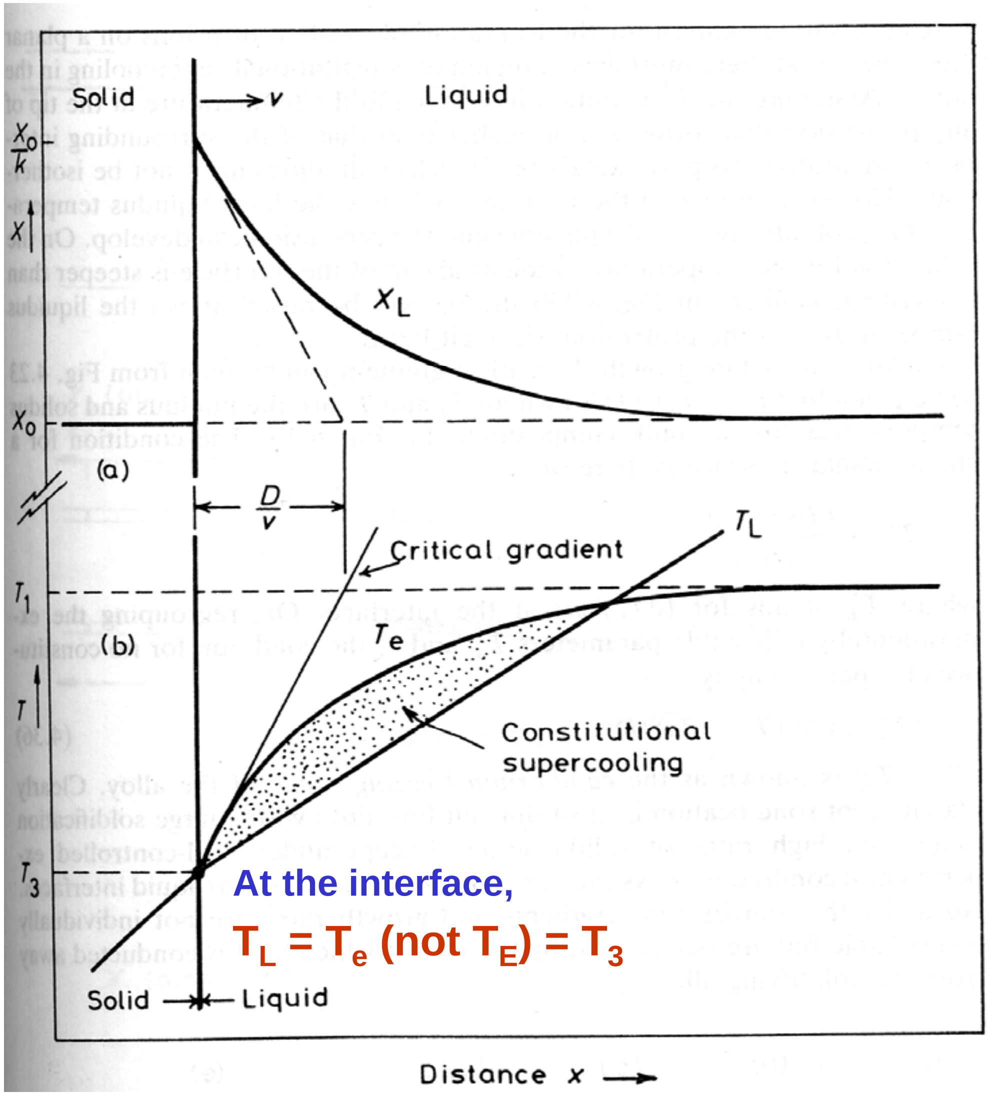

At the interface,

$T_L = T_e$ (not T_E) $= T_3$

Condition for a stable planar interface

$T_L' > (T_1 - T_3)/(D/v)$

$T_L'/v > (T_1 - T_3)/D$

Fig. 4.23 The origin of constitutional supercooling ahead of a planar solidification front. (a) Composition profile across the solid/liquid interface during steady-state solidification. The dashed line shows dX_L/dx at the S/L interface. (b) The temperature of the liquid ahead of the solidification front follows line T_L. The equilibrium liquidus temperature for the liquid adjacent to the interface varies as T_e. Constitutional supercooling arises when T_L lies under the critical gradient.

Contents for today's class

4.3 Alloy solidification

- Solidification of single-phase alloys
- Eutectic solidification
- Off-eutectic alloys
- Peritectic solidification

4.4 Solidification of ingots and castings

- Ingot structure
- Segregation in ingot and castings
- Continuous casting

4.6 Solidification during quenching from the melt

4.3.2 Eutectic Solidification

Normal eutectic

Fig. 4.30 Rod-like eutectic. Al$_6$Fe rods in Al matrix. Transverse section. Transmission electron micrograph (x 70000).

Anomalous eutectic

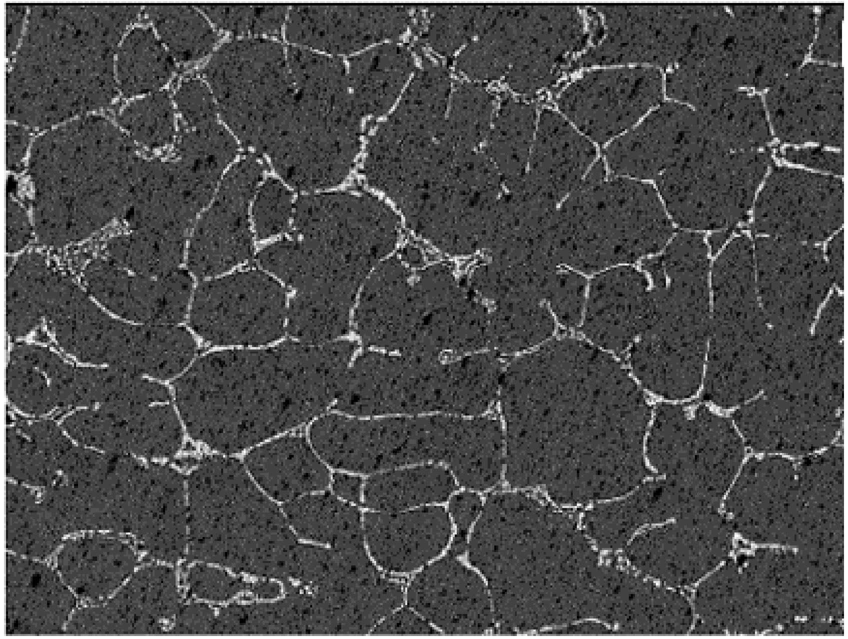

The microstructure of the Pb-61.9%Sn (eutectic) alloy presented a coupled growth of the (Pb)/bSn eutectic. There is a remarkable change in morphology increasing the degree of undercooling with transition from regular lamellar to anomalous eutectic.

http://www.matter.org.uk/solidification/eutectic/anomalous_eutectics.htm

4.3.2 Eutectic Solidification

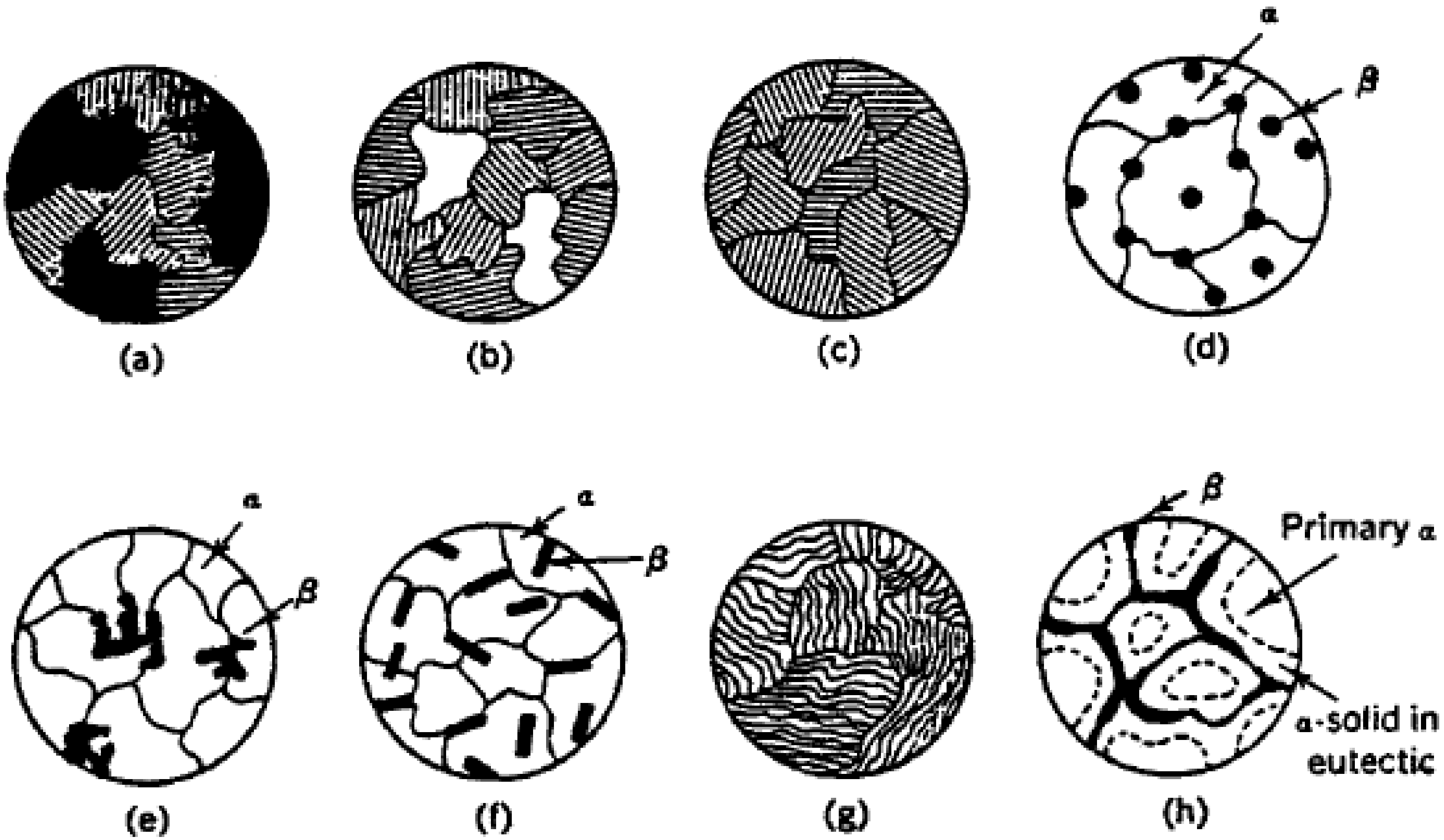

Fig. 14 Schematic representation possible in eutectic structures. (a), (b) and (c) are alloys shown in fig. 13; (d) nodular; (e) Chinese script; (f) acicular; (g) lamellar; and (h) divorced.

4.3.2 Eutectic Solidification (Thermodynamics)

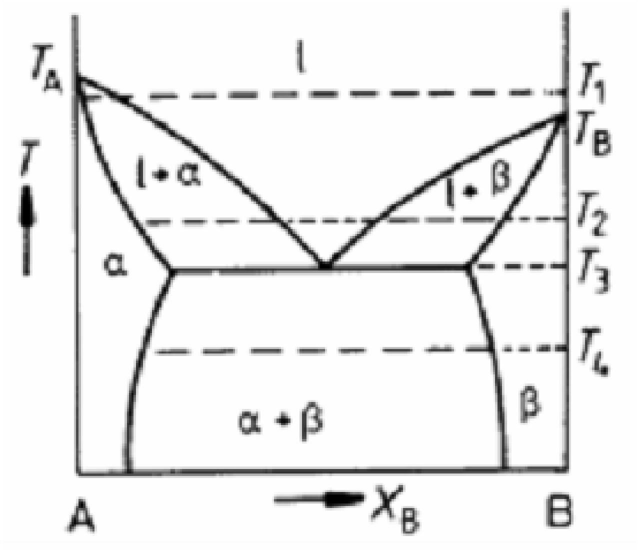

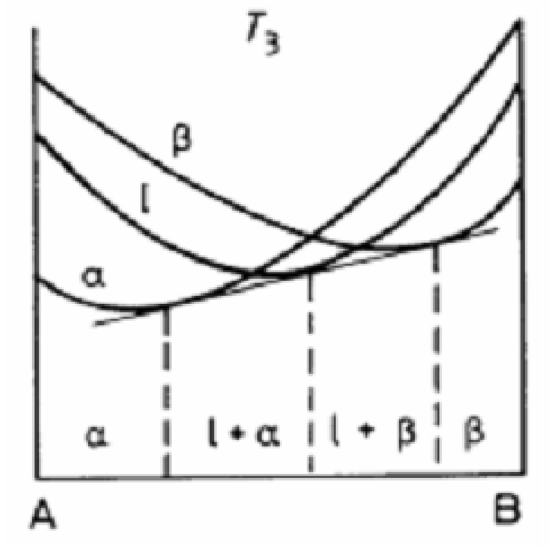

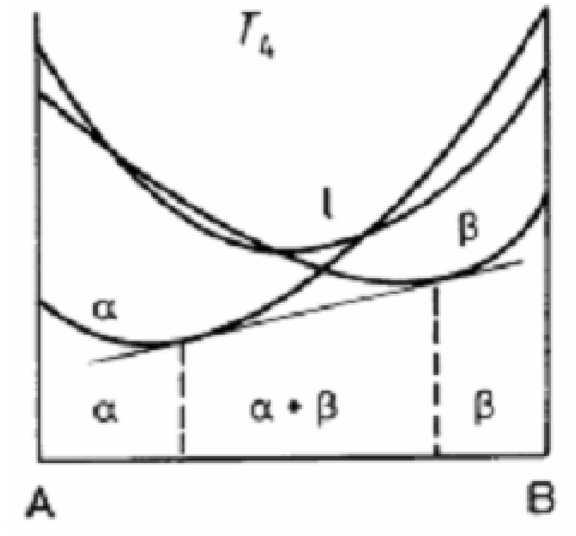

Plot the diagram of Gibbs free energy vs. composition at T_3 and T_4.

What is the driving force for the eutectic reaction (L →α + β) at T_4 at C_{eut}?

What is the driving force for nucleation of α and β?

Eutectic Solidification (Kinetics)

If α is nucleated from liquid and starts to grow, what would be the composition at the interface of α/L determined?

→ rough interface & local equilibrium

How about at β/L? Nature's choice?

interlamellar spacing →

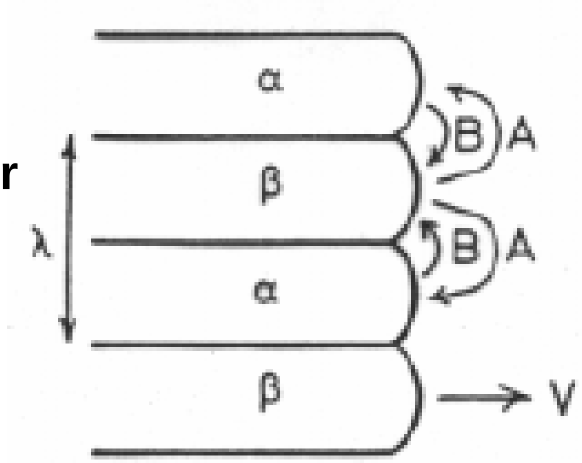

What would be a role of the curvature at the tip?

→ Gibbs-Thomson Effect

Eutectic Solidification

How many α/β interfaces per unit length? $\rightarrow 1/\lambda \times 2$

For an interlamellar spacing, λ, there is a total of (2/ λ) m^2 of α/β interface per m^3 of eutectic.

$$\Delta G = \Delta \mu \cong \frac{L \Delta T}{T_m}$$

Driving force for nucleation

$$\rightarrow \Delta G = \Delta \mu = \frac{2\gamma}{\lambda} \times V_m$$

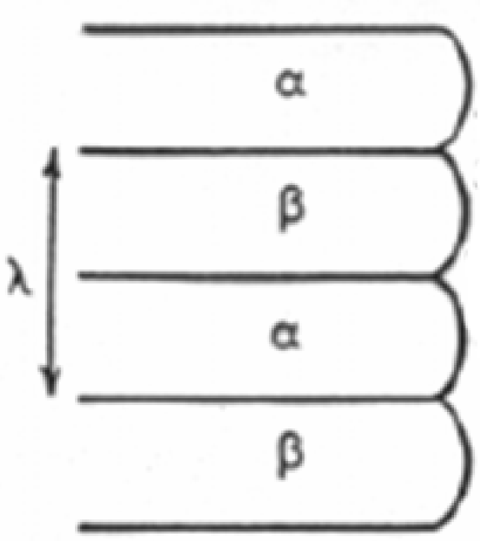

$$\lambda \rightarrow \infty \; , \quad \Delta G(\infty) = \Delta \mu = \frac{\Delta H \, \Delta T_0}{T_E}$$

$$\Delta G(\lambda) = ? = -\Delta G(\infty) + \frac{2\gamma V_m}{\lambda}$$

What would be the minimum λ?

Critical spacing, $\lambda^* : \Delta G(\lambda^*) = 0$

$$\Delta G(\infty) = \frac{2\gamma V_m}{\lambda^*}$$

$$\lambda^* = -\frac{2 T_E \gamma V_m}{\Delta H \, \Delta T_0}$$

$$cf)\; r^* = \frac{2\gamma_{SL}}{\Delta G_V} = \left(\frac{2\gamma_{SL} T_m}{L_V}\right) \frac{1}{\Delta T}$$

L_V : *latent heat per unit volume*

$L = \Delta H = H^L - H^S$

$$\lambda^* = -\frac{2T_E\gamma V_m}{\Delta H \Delta T_0} \rightarrow \textit{identical to critical radius}$$

Gibbs-Thomson effect in a ΔG-composition diagram?

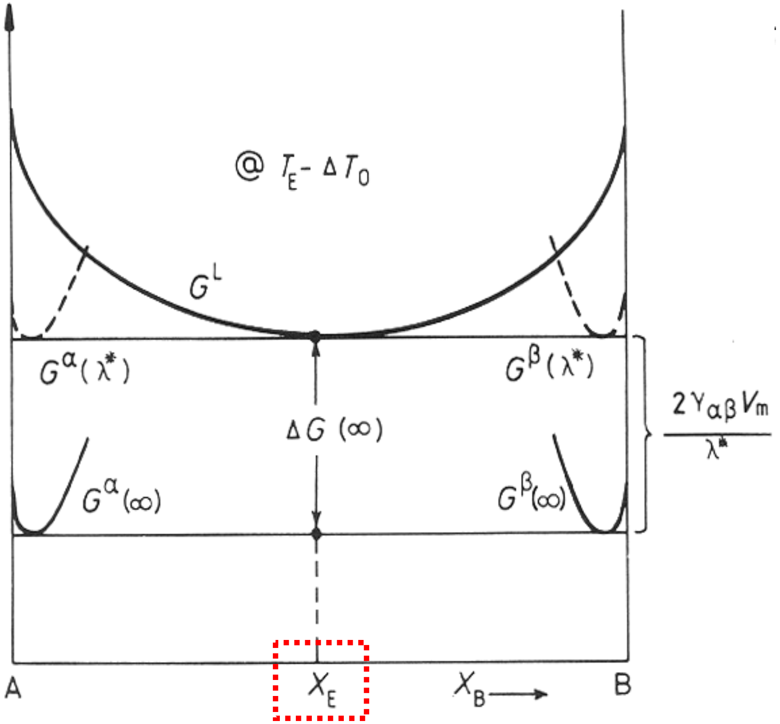

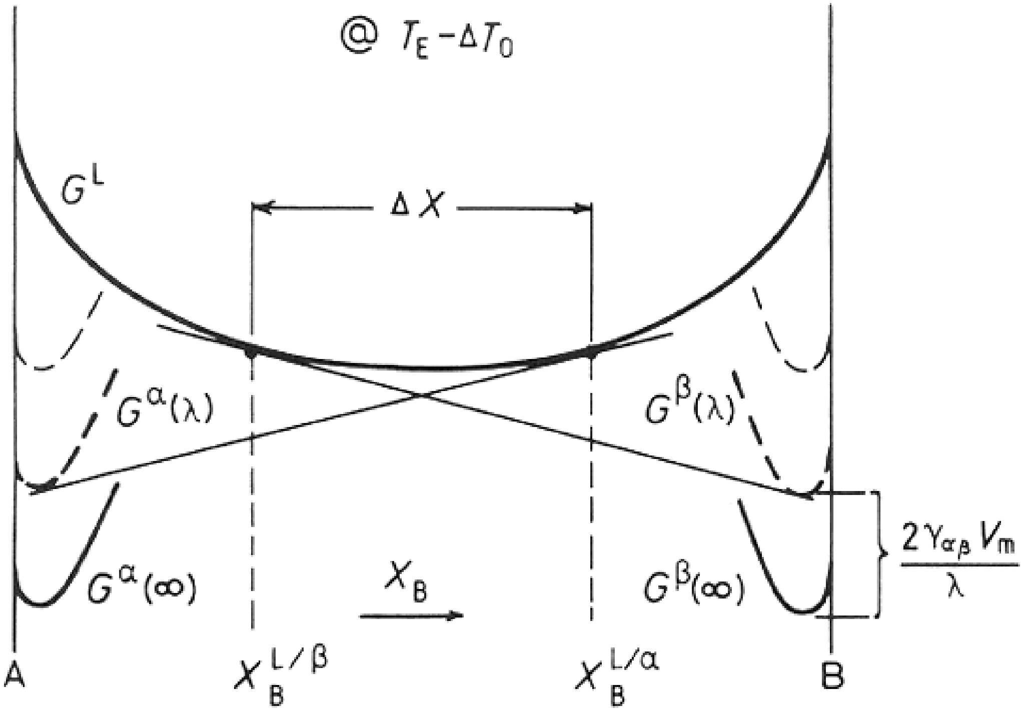

β 상과 국부적
평형 이루는
액상의 조성

<

α 상과 국부적
평형 이루는
액상의 조성

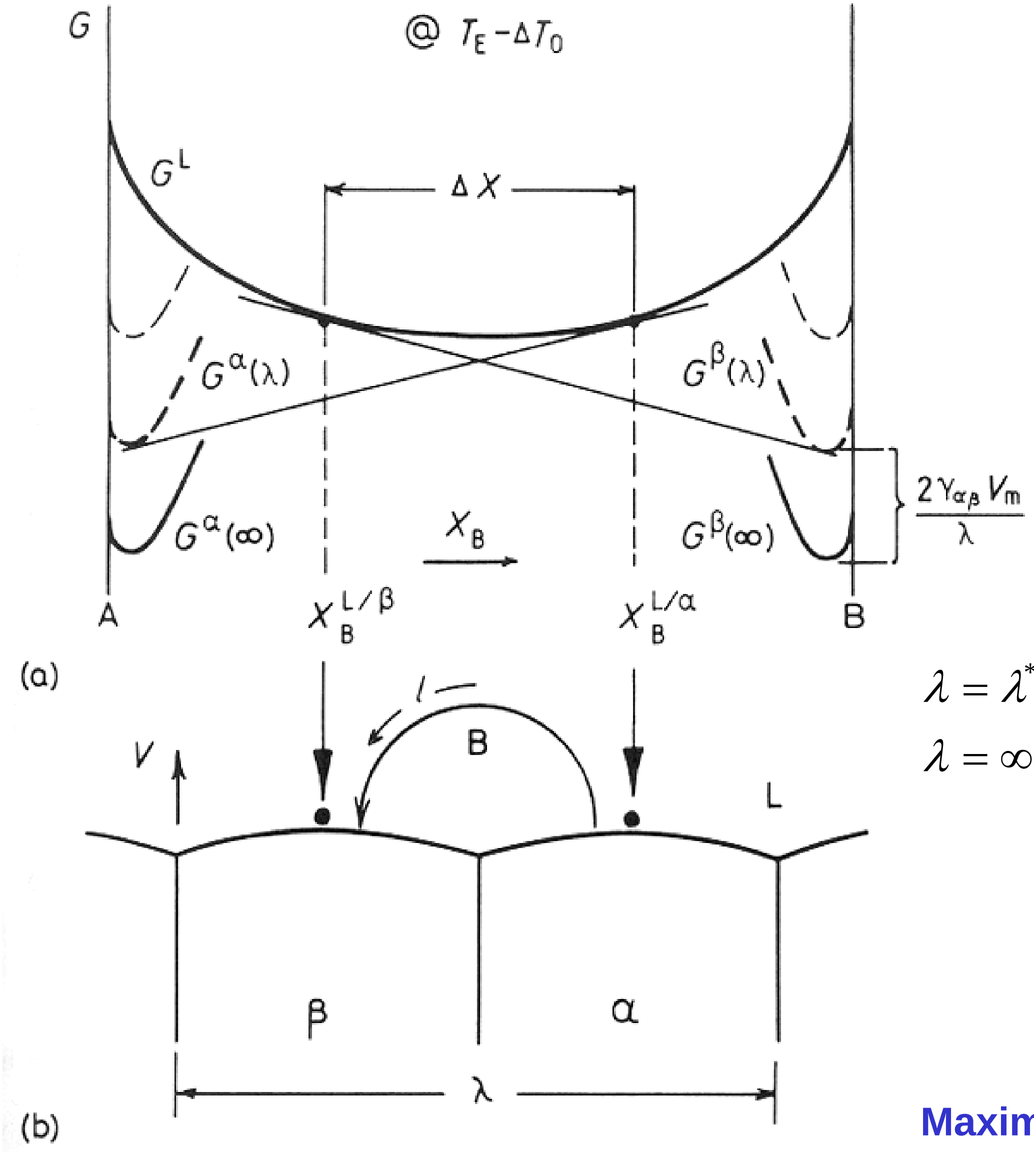

공정의 성장속도 ***v***

→ 액상을 통한 용질이동과 비례

→ 성장 확산 제어

$$\boxed{v \propto D\frac{dC}{dl} \propto (X_B^{L/\alpha} - X_B^{L/\beta}) \quad \propto \ 1/\text{유효확산거리} \cdots 1/\lambda}$$

$$\boxed{v = k_1 D\frac{\Delta X}{\lambda}}$$

$$\lambda = \lambda^*, \Delta X = 0$$

$$\lambda = \infty, \Delta X = \Delta X_0$$

$$\boxed{\Delta X = \Delta X_0\left(1 - \frac{\lambda^*}{\lambda}\right)}$$

$$\Delta X_0 \propto \Delta T_0$$

$$\boxed{v = k_2 D\frac{\Delta T_0}{\lambda}\left(1 - \frac{\lambda^*}{\lambda}\right)}$$

Maximum growth rate at a fixed ΔT_0 → $\boxed{\lambda = 2\lambda^*}$

Fig. 4.33 (a) Molar free energy diagram at (T_E - ΔT_0) for the case λ * < λ < ∞ , showing the composition difference available to drive diffusion through the liquid (ΔX). (b) Model used to calculate the growth rate.

Corresponding location at phase diagram?

$$\Delta T_0 = \Delta T_r + \Delta T_D$$

$$\Delta G_{total} = \Delta G_r + \Delta G_D$$

$$\Delta G_r = \frac{2\gamma_{\alpha\gamma} V_m}{\lambda}$$

$\rightarrow$ *free energy dissipated in forming* α/β *interfaces*

$\Delta G_D \rightarrow$ *free energy dissipated in diffusion*

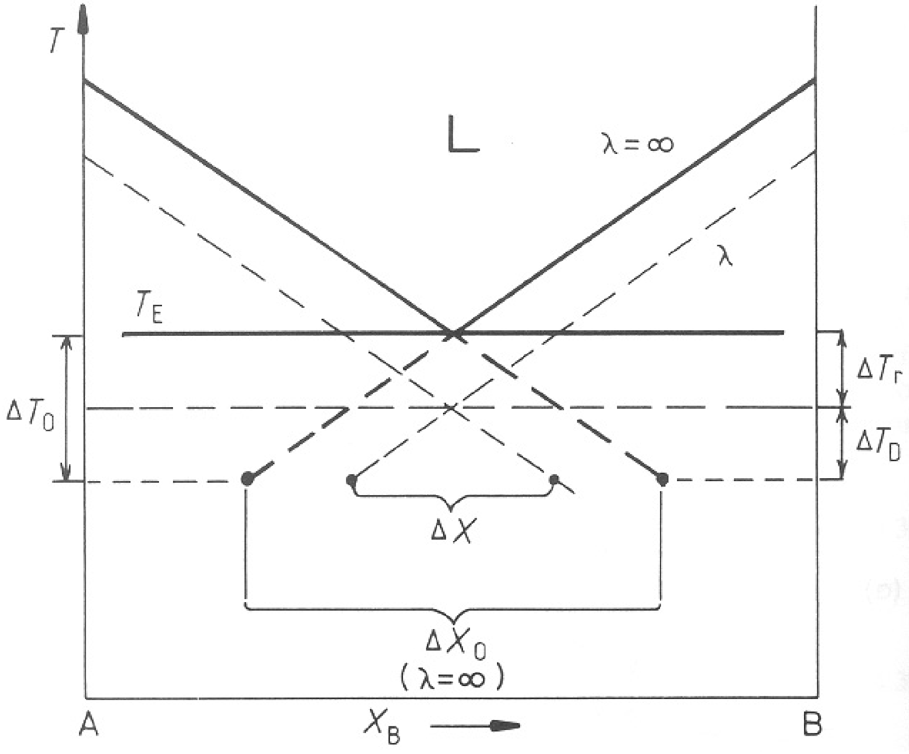

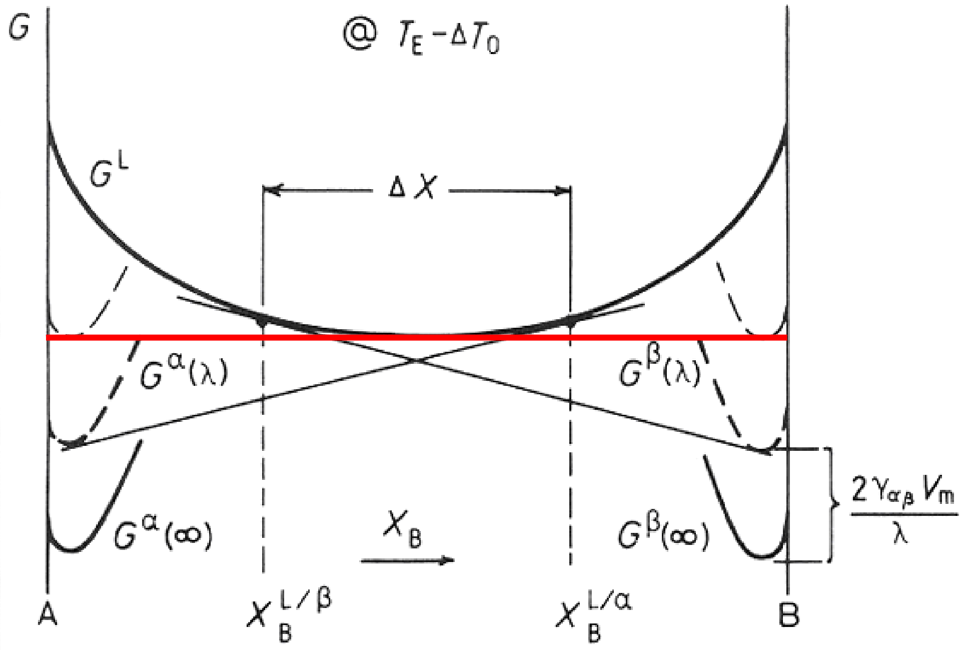

Fig. 4.34 Eutectic phase diagram showing the relationship between ΔX and ΔX_0 (exaggerated for clarity)

$$v = k_2 D \frac{\Delta T_0}{\lambda}\left(1 - \frac{\lambda^*}{\lambda}\right)$$

Maximum growth rate at a fixed $\Delta T_0 \rightarrow$ $\boxed{\lambda = 2\lambda^*}$

$$v_0 = k_2 D \Delta T_0 / 4\lambda^*$$

$$\lambda^* = -\frac{2T_E \gamma V_m}{\Delta H \Delta T_0}$$ 로 부터, $\Delta T_0 \propto 1/\lambda^*$

$\lambda = \lambda_0$ 인 경우,

$$v_0 \lambda_0^2 = k_3$$

$$\frac{v_0}{(\Delta T_0)^2} = k_4$$

$$\Delta T_0 = \Delta T_r + \Delta T_D$$

계면 곡률효과 극복 과냉도   확산위해 충분한 조성차주기 위한 과냉

$\Delta T_D \rightarrow$ α층의 중간부터 β층의 중간까지 변화

$\Delta T_0 = const$ 계면 등은 항상 등온

ΔT_r 로 극복해야 함 → 계면의 곡률을 따라 변화

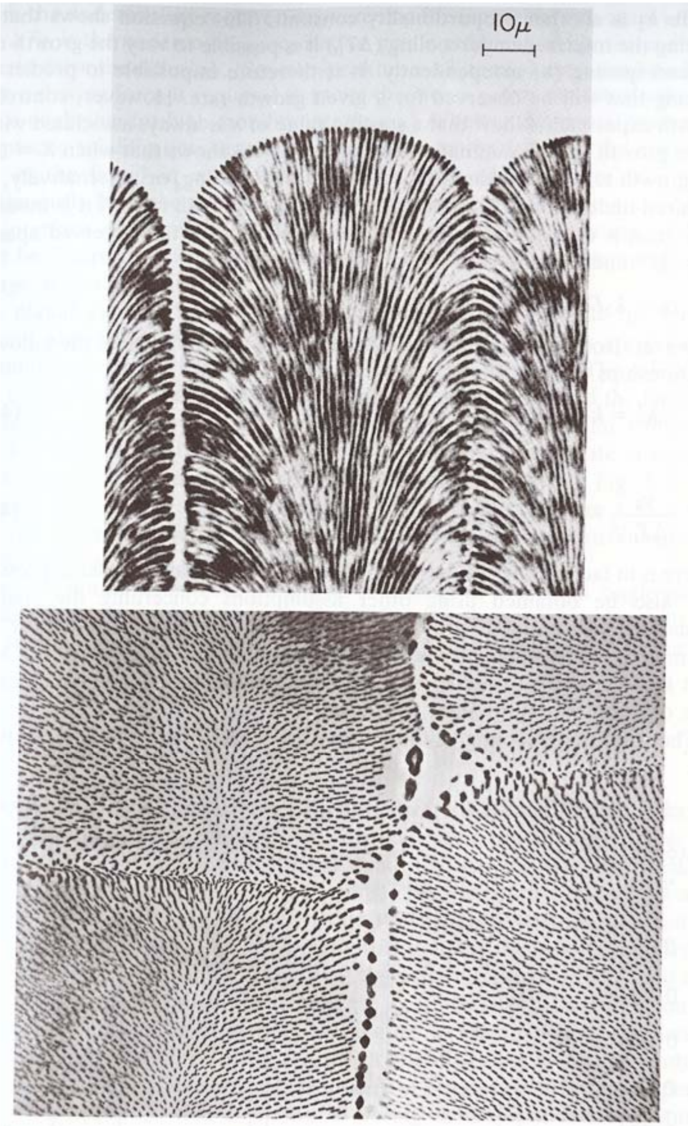

4.3.3 Off-eutectic Solidification

primary α + eutectic lamellar

- Primary **α** dendrites form at T_1. Rejected solute increases X_L to X_E; eutectic solidification follows.
- Coring : primary **α** (low solute) at T_1 and the eutectic (high solute) at T_E.

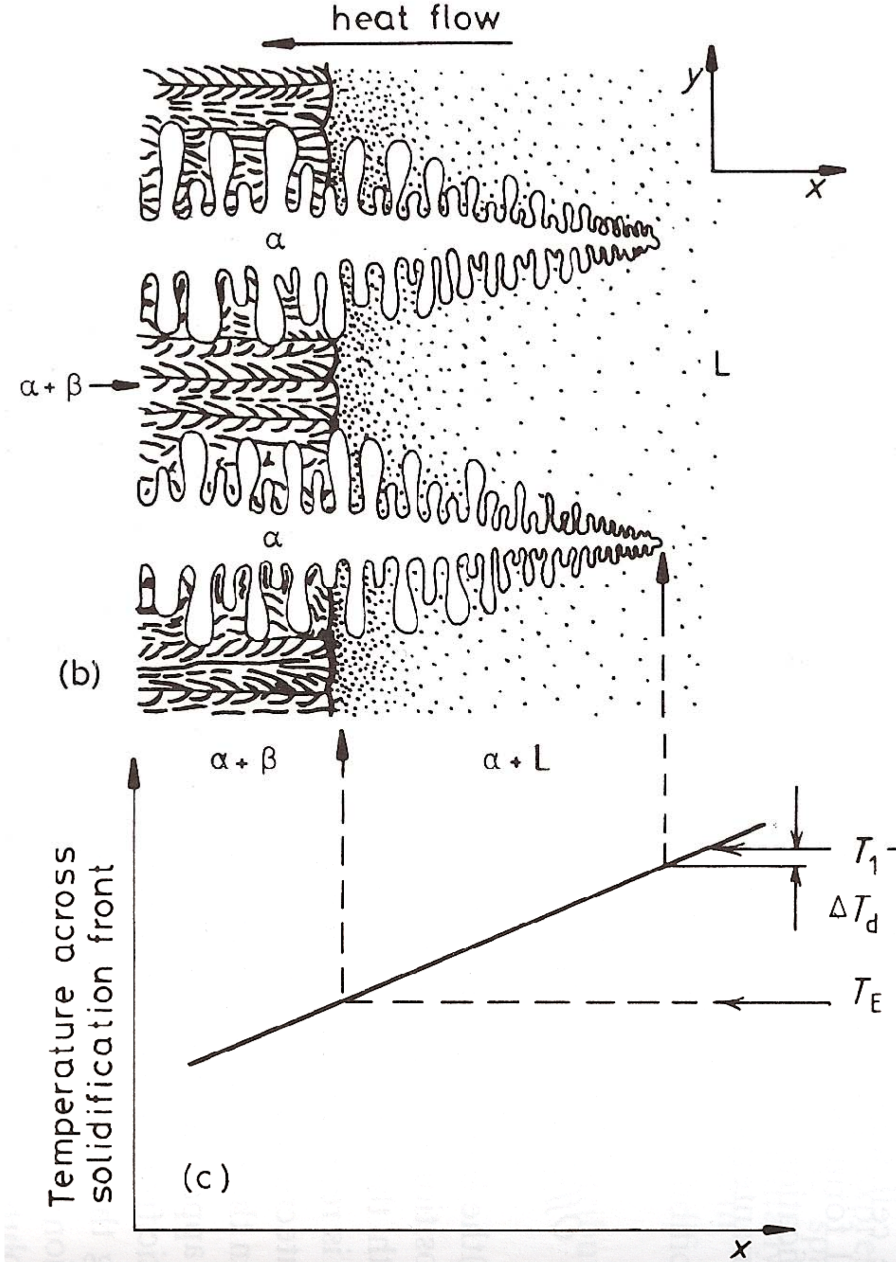

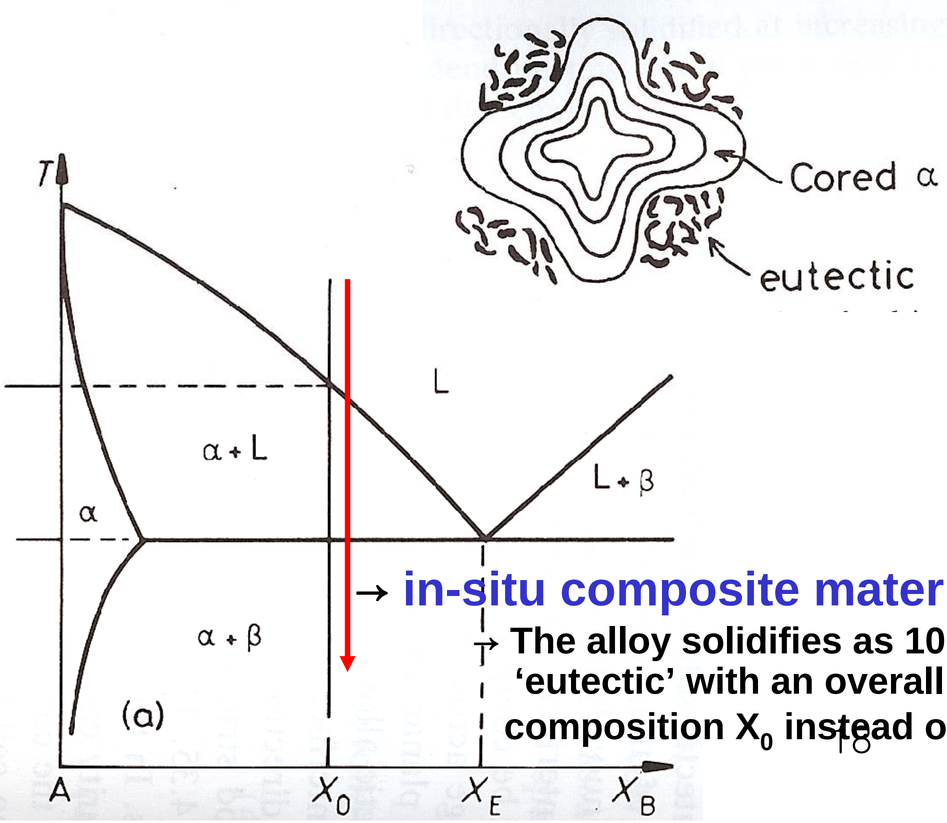

→ **in-situ composite materials**

→ **The alloy solidifies as 100% 'eutectic' with an overall composition X_0 instead of X_E.**

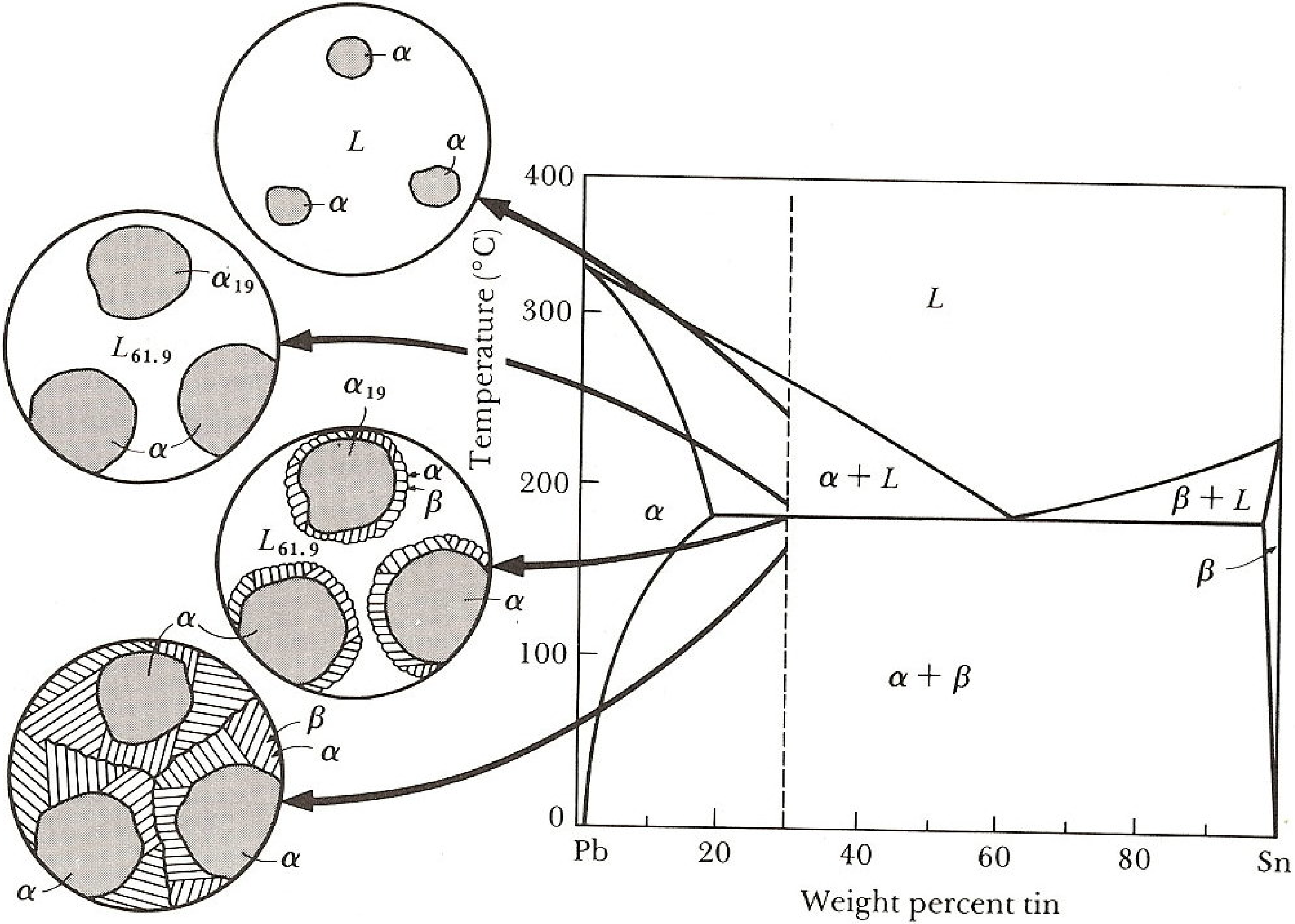

FIGURE 10-12 The solidification and microstructure of a hypoeutectic alloy (Pb-30% Sn).

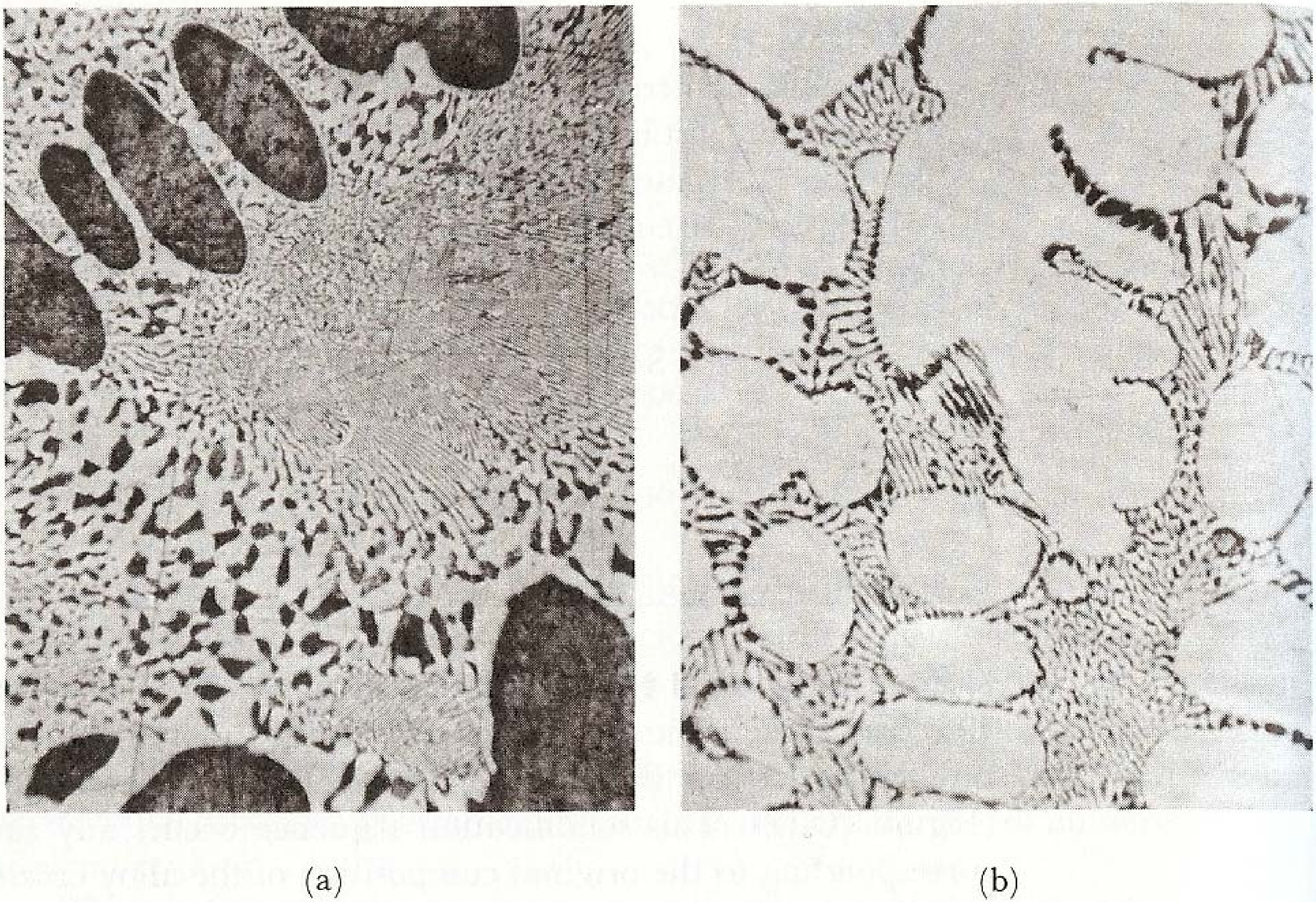

(a) (b)

FIGURE 10-13 (a) A hypoeutectic lead-tin alloy. (b) A hypereutectic lead-tin alloy. The dark constituent is the lead-rich solid α, the light constituent is the tin-rich solid β, and the fine plate structure is the eutectic (× 400).

4.3.4 Peritectic Solidification

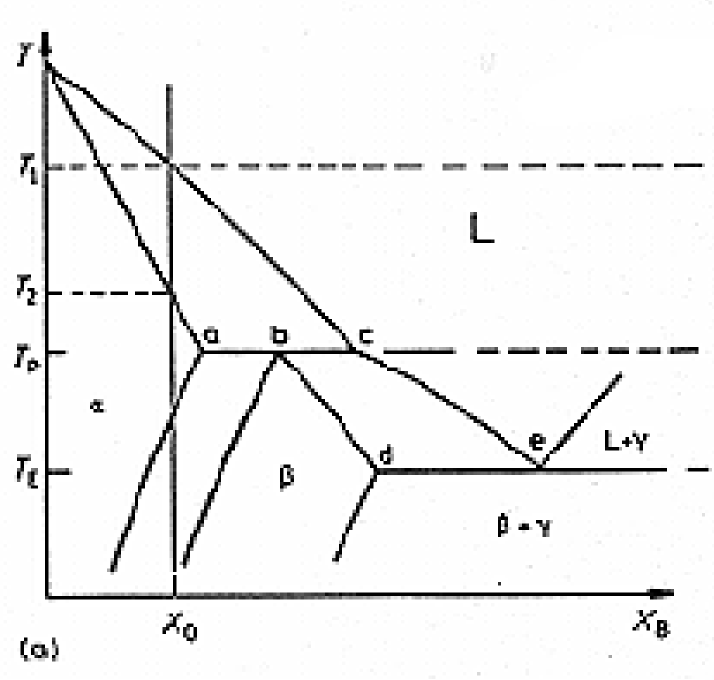

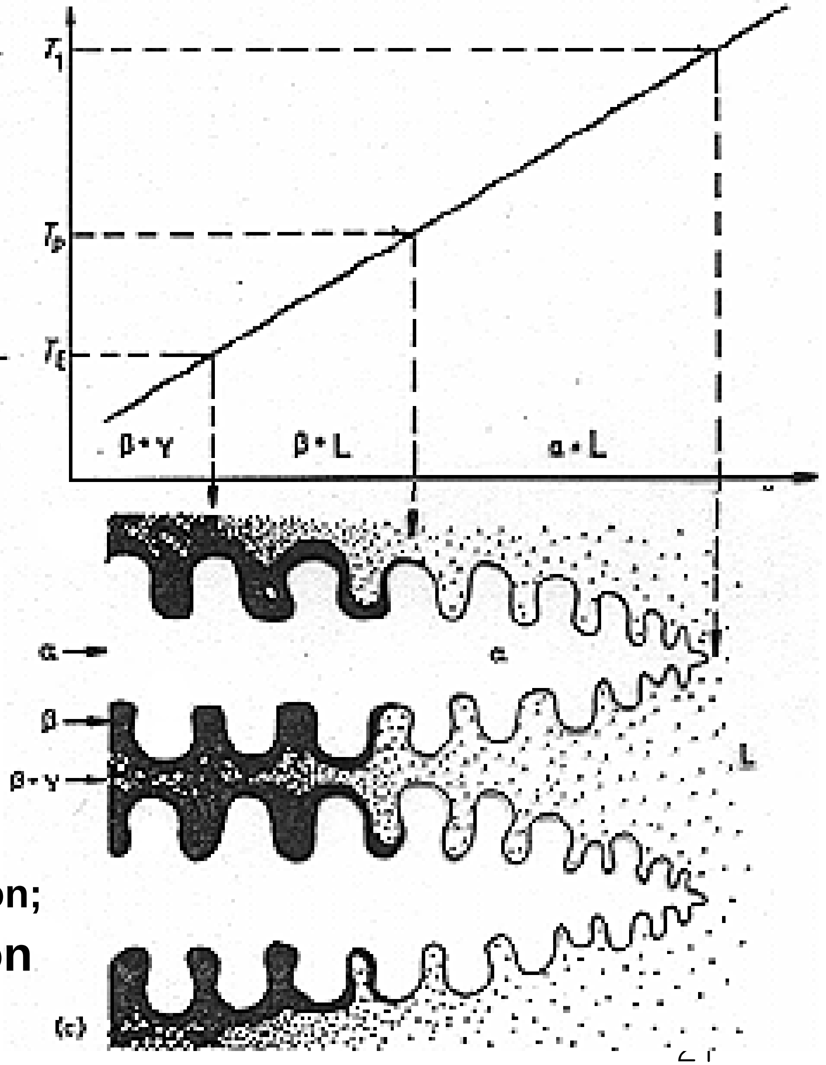

- **L + α → β , difficult to complete.**

- **α dendrites first form at T_1;**
  Liquid reaches the composition ‘c’;
  β forms as the result of the peritectic reaction;
  α coring is isolated from further reaction
  finally β + γ eutectic forms.

Solidification and microstructure

that develop as a result of the peritectic reaction

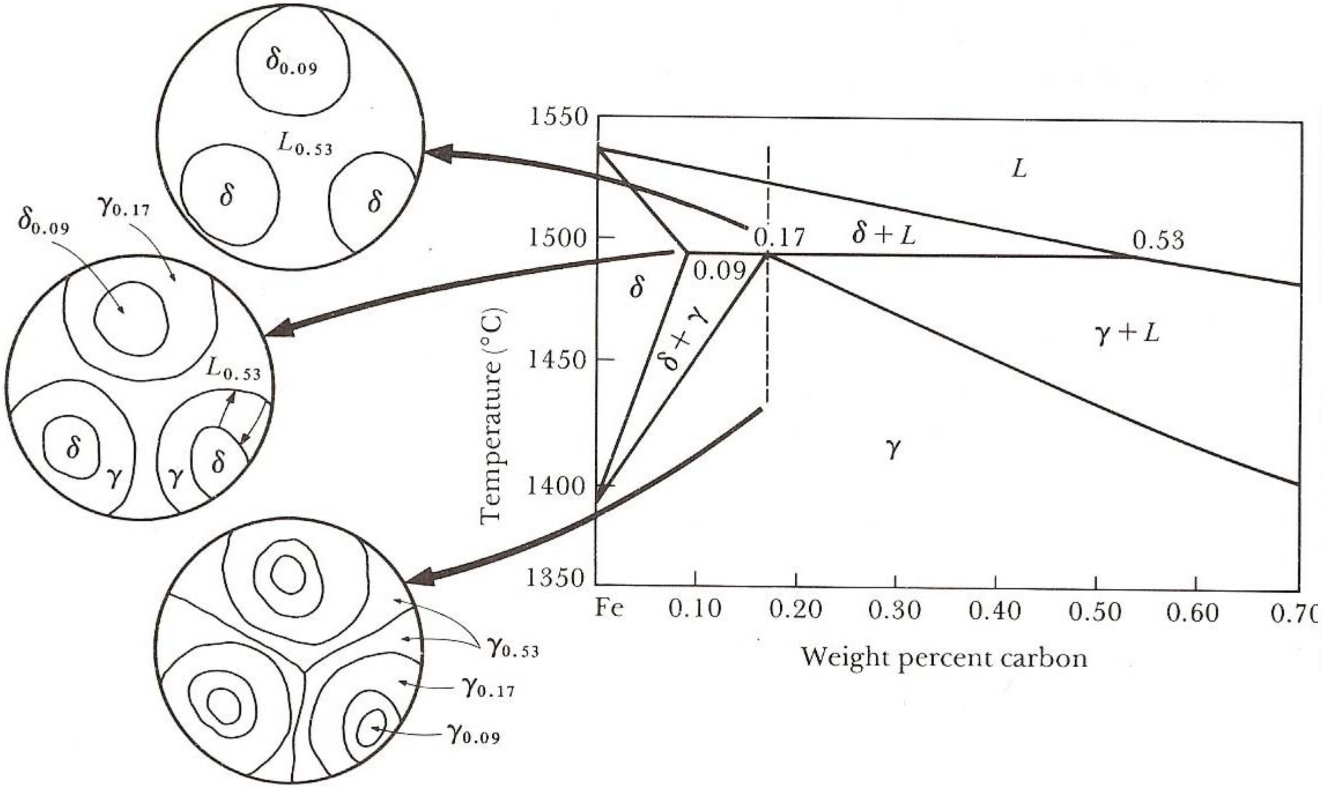

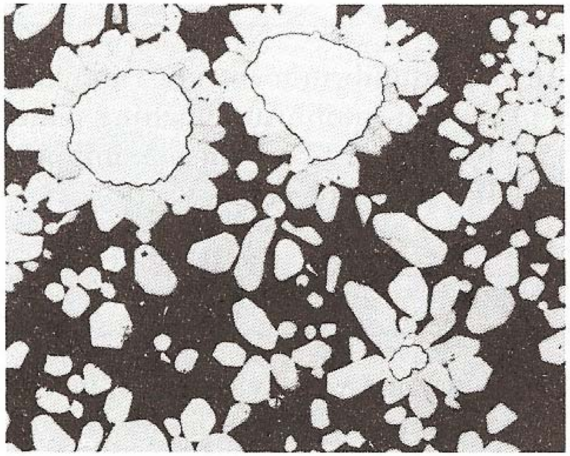

FIGURE 10-24 The peritectic reaction in a Cd-10% Cu alloy begins when rounded

4.4 Solidification of Ingots and Castings

주조 후 압연, 압출 또
는 단조 등에 의해 가공
할 것 >> blank (작은 것)

주조된 제품이 최종 모양
을 유지하거나 혹은 기계
가공에 의해 최종 모양으
로 된 것

Ingot Structure

- Chill zone
- Columnar zone
- Equiaxed zone

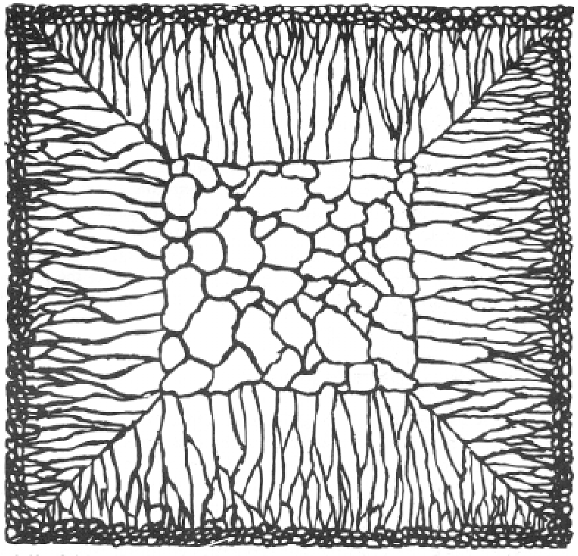

Chill zone

- Solid nuclei form on the mould wall and begin to grow into the liquid.

- As the mould wall warms up it is possible for many of these solidified crystals to break away from the wall under the influence of the turbulent melt.

Columnar zone

After pouring the temperature gradient at the mould walls decreases and the crystals in the chill zone grow dendritically in certain crystallographic directions, e.g. <100> in the case of cubic metals.

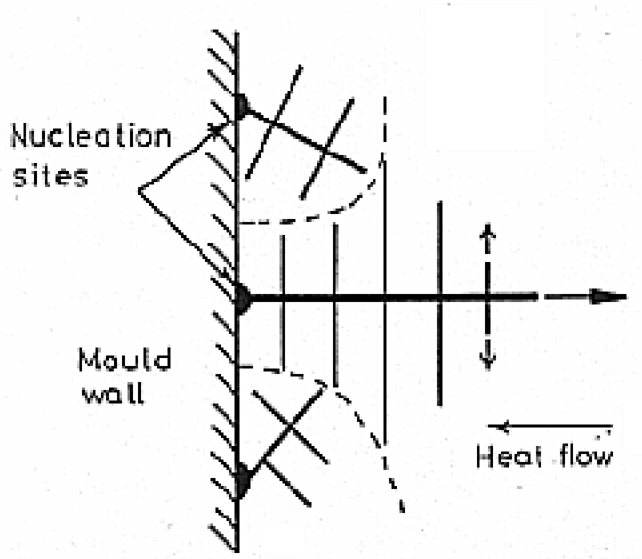

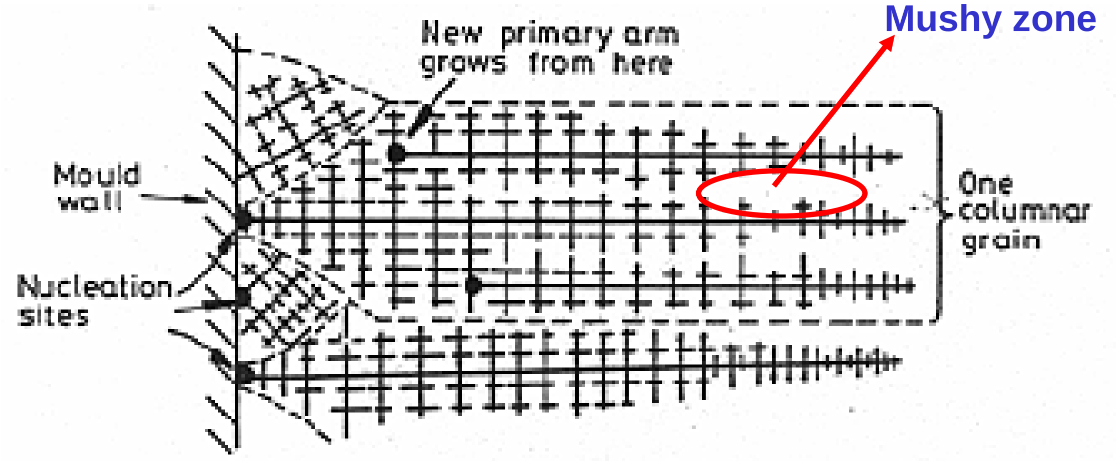

Fig. 4.41 Competitive growth soon after pouring. Dendrites with primary arms normal to the mould wall, i.e. parallel to the maximum temperature gradient, outgrow less favorably oriented neighbors.

Fig. 4.42 Favorably oriented dendrites develop into columnar grains. Each columnar grain originates from the same heterogeneous nucleation site, but can contain many primary dendrite arms.

1차 가지 성장 방향 변화

열전도 방향 → 결정학적 우선 방향

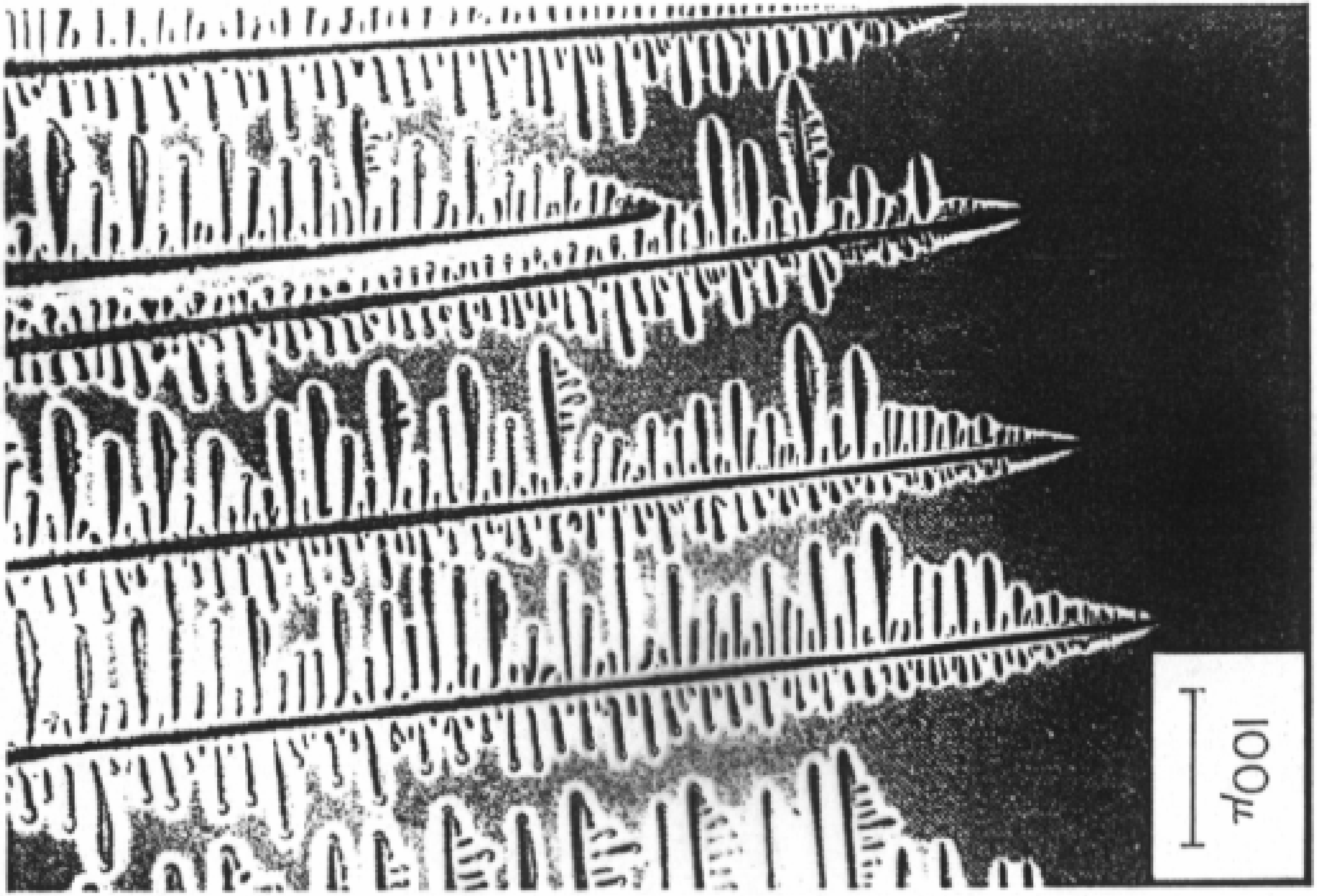

Fig. 4.28 Columnar dendrites in a transparent organic alloy.

(After K.A. Jackson in Solidification, American Society for Metals, 1971, p. 121.)

Equiaxed zone

The equiaxed zone consists of equiaxed grains randomly oriented in the centre of the ingot. An important origin of these grains is thought to be melted-off dendrite side-arms. + convection current

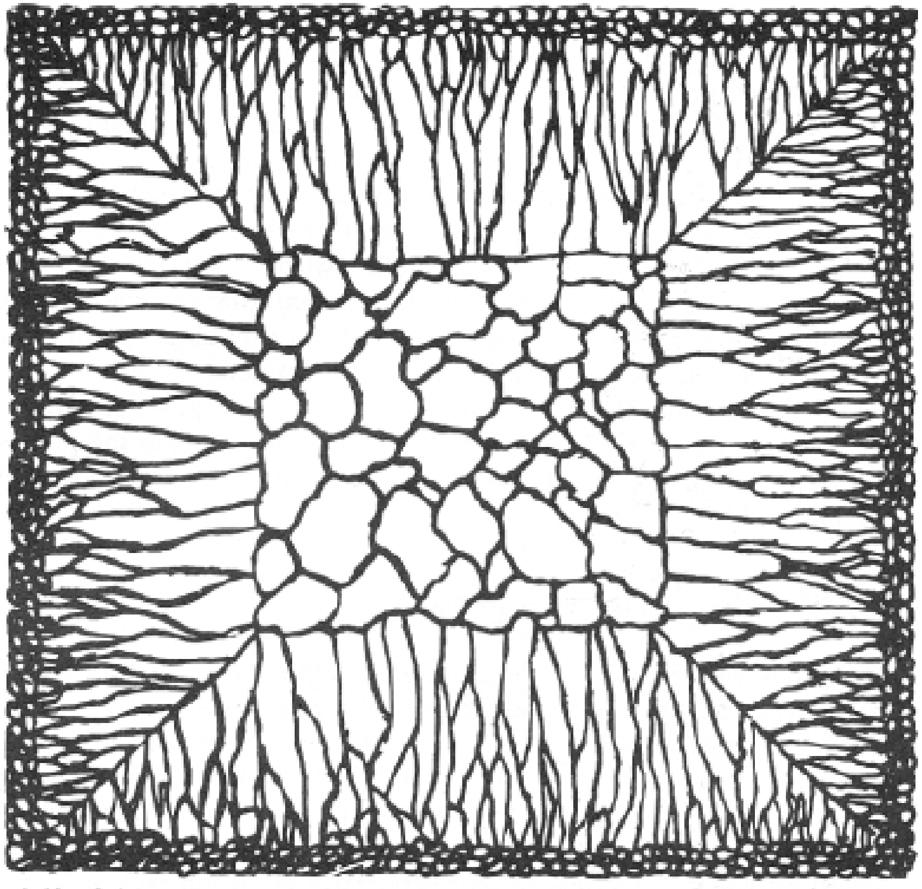

Fig. 4.40 Schematic cast grain structure.

(After M.C. Flemings, Solidification Processing, McGraw-Hill, New York, 1974.)

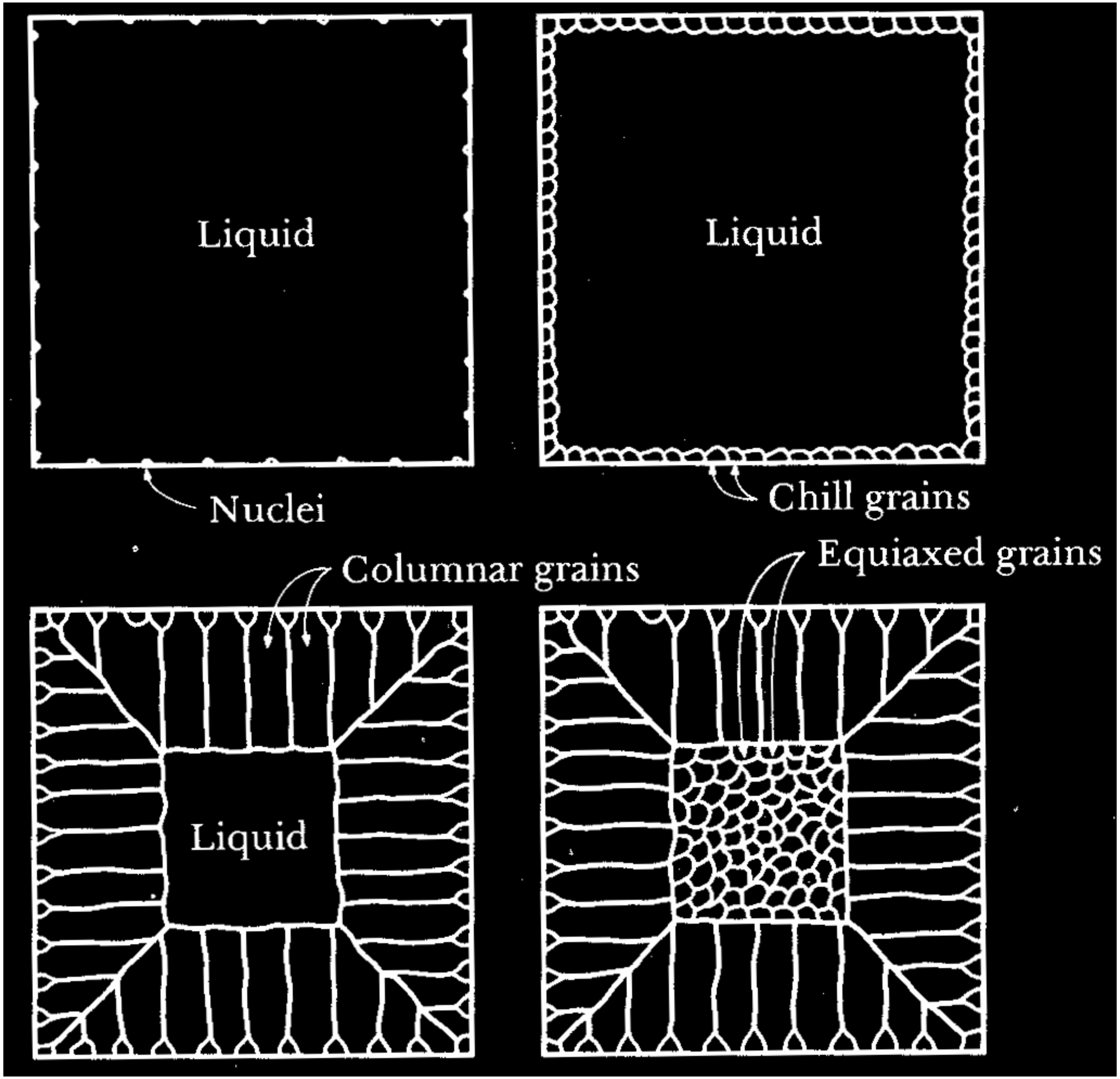
Liquid
Liquid
Nuclei
Chill grains
Columnar grains
Equiaxed grains
Liquid

Shrinkage effect

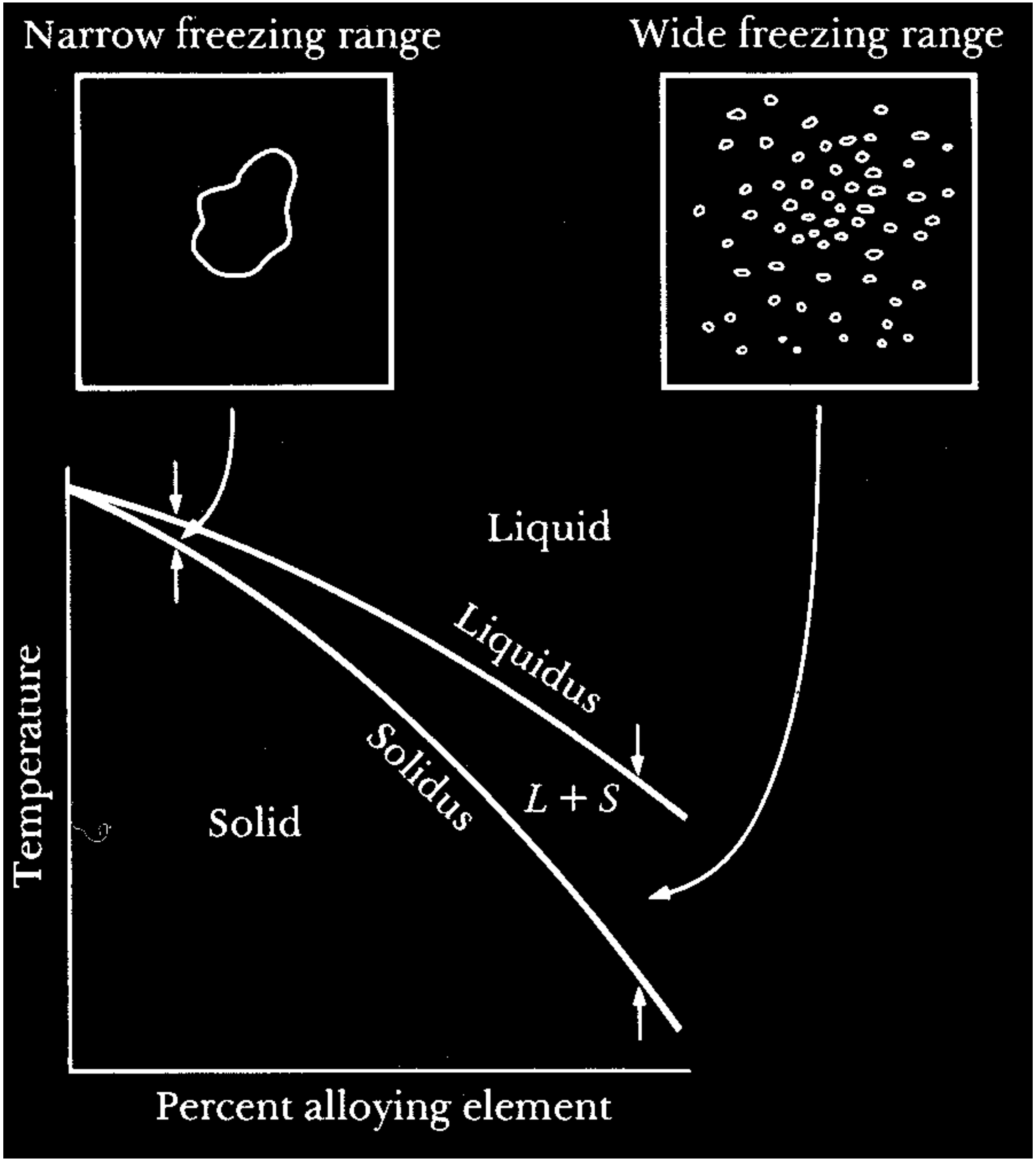

4.4.2 Segregation in Ingots and Castings

- Macrosegregation :
  Composition changes over distances comparable to the size of the specimen.

- Microsegregation :
  Occur on the scale of the secondary dendrite arm spacing.

Four important factors **that can lead to** macrosegregation

- **Shrinkage due to solidification and thermal contraction.**
- **Density differences in the interdendritic liquid.**
- **Density differences between the solid and liquid**
- **Convection currents driven by temperature-induced density differences in the liquid.**

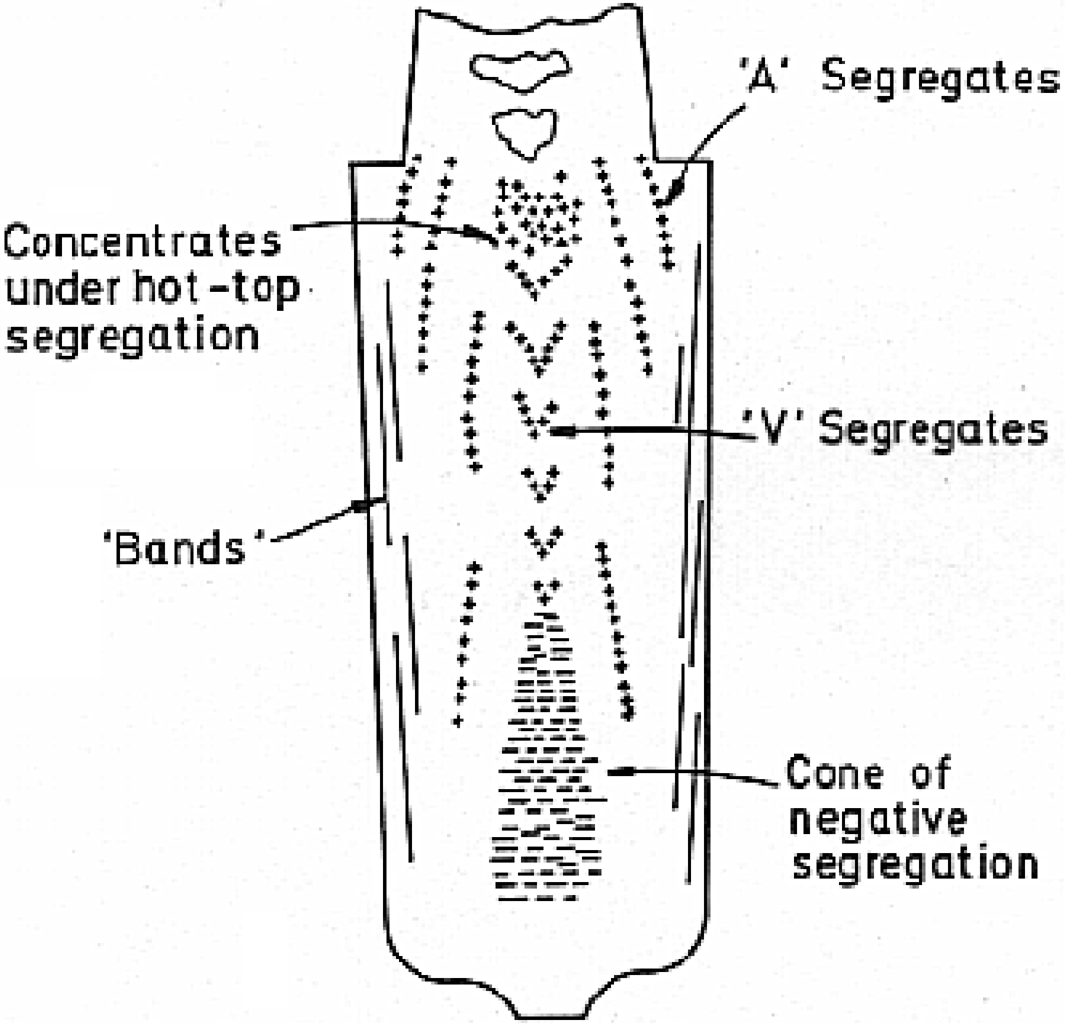

역편석: 주상정 수지상이 두꺼워지면 용질이 농축된 액상 ($k<1$인 경우)이 수축을 보충하기 위해 수지상 사이로 다시 흘러들어온다.

음의 편석: 등축결정 형성시 중력효과에 의함. 일반적으로 고상은 액상보다 밀도 높고, $k<1$ 이라면 고상의 조성은 본래의 조성보다 낮은 조성을 가짐.

Fig. 4.43 Segregation pattern in a large killed steel ingot. + positive, - negative segregation. (After M.C. Flemings, Scandinavian Journal of Metallurgy 5 (1976) 1.)

4.4.3 continuous casting

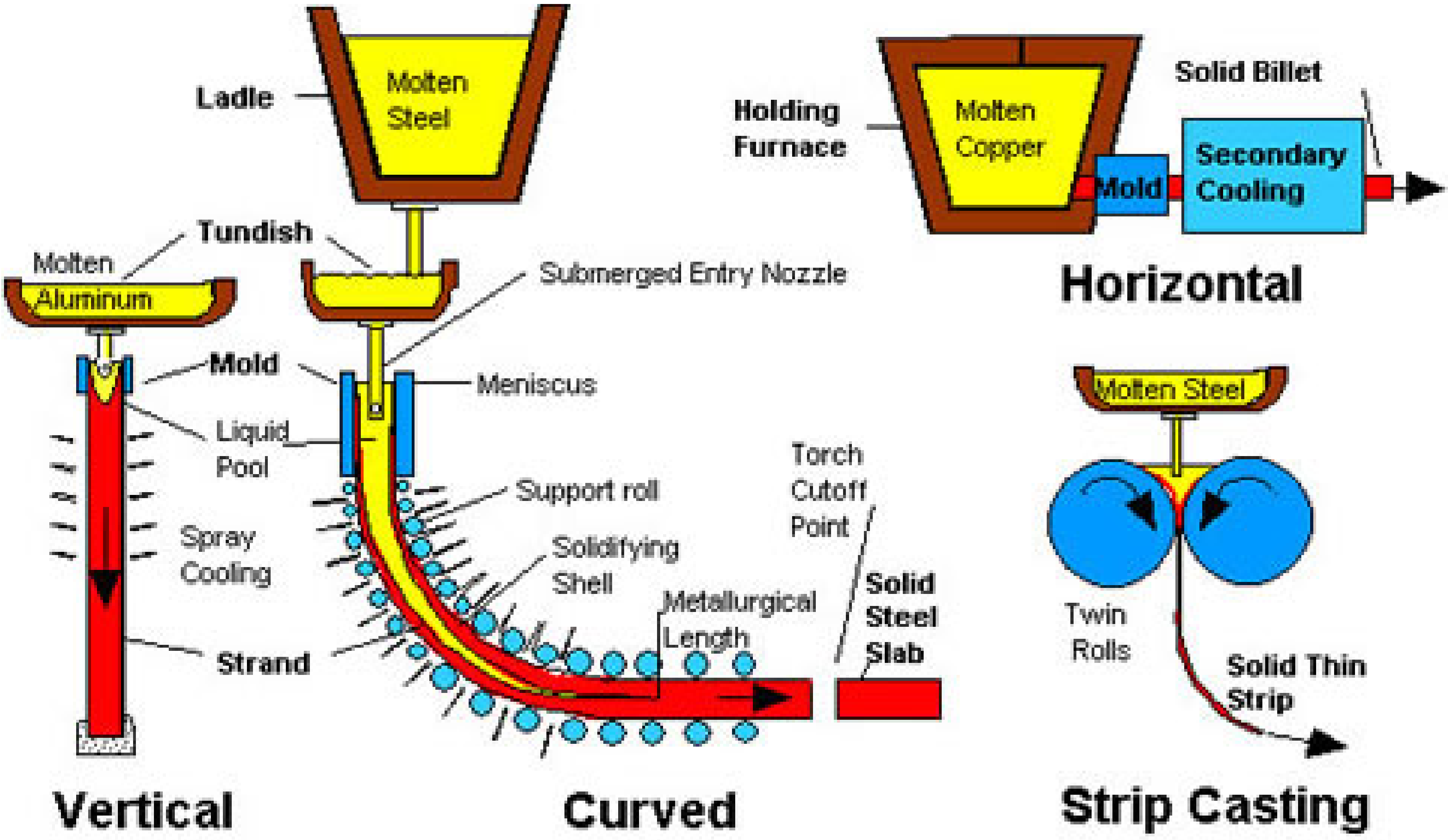

4.4.3 continuous casting

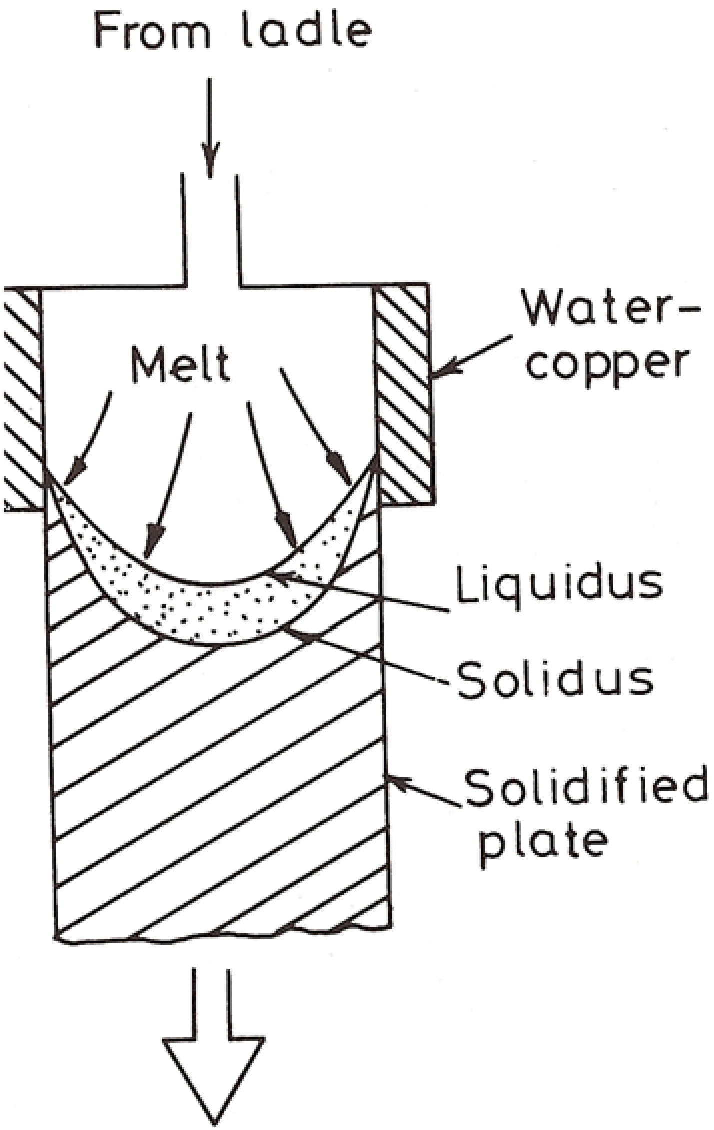

Schematic illustration of a continuous casting process.

4.4.3 continuous casting

4.4.3 continuous casting

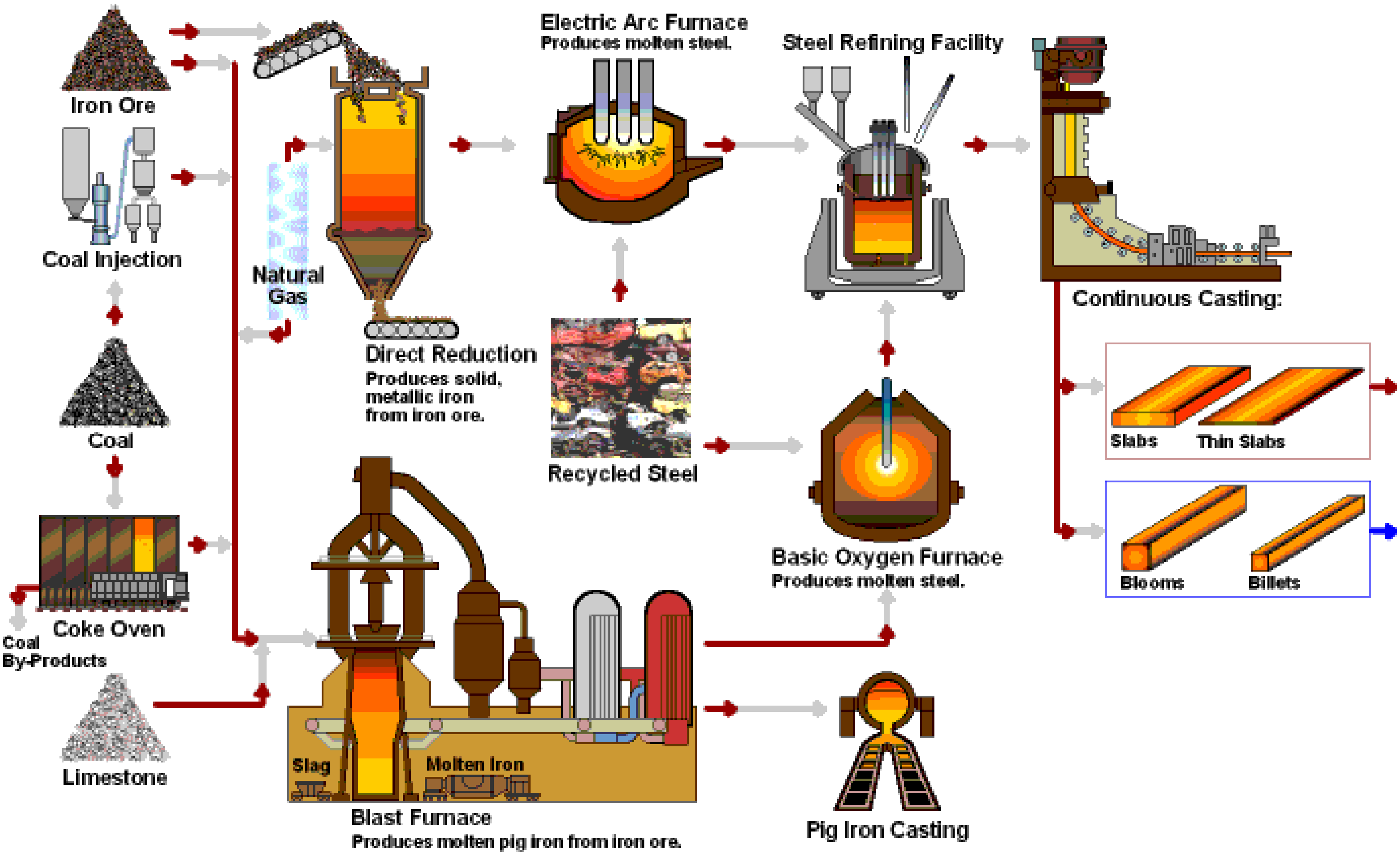

4.4.3 continuous casting

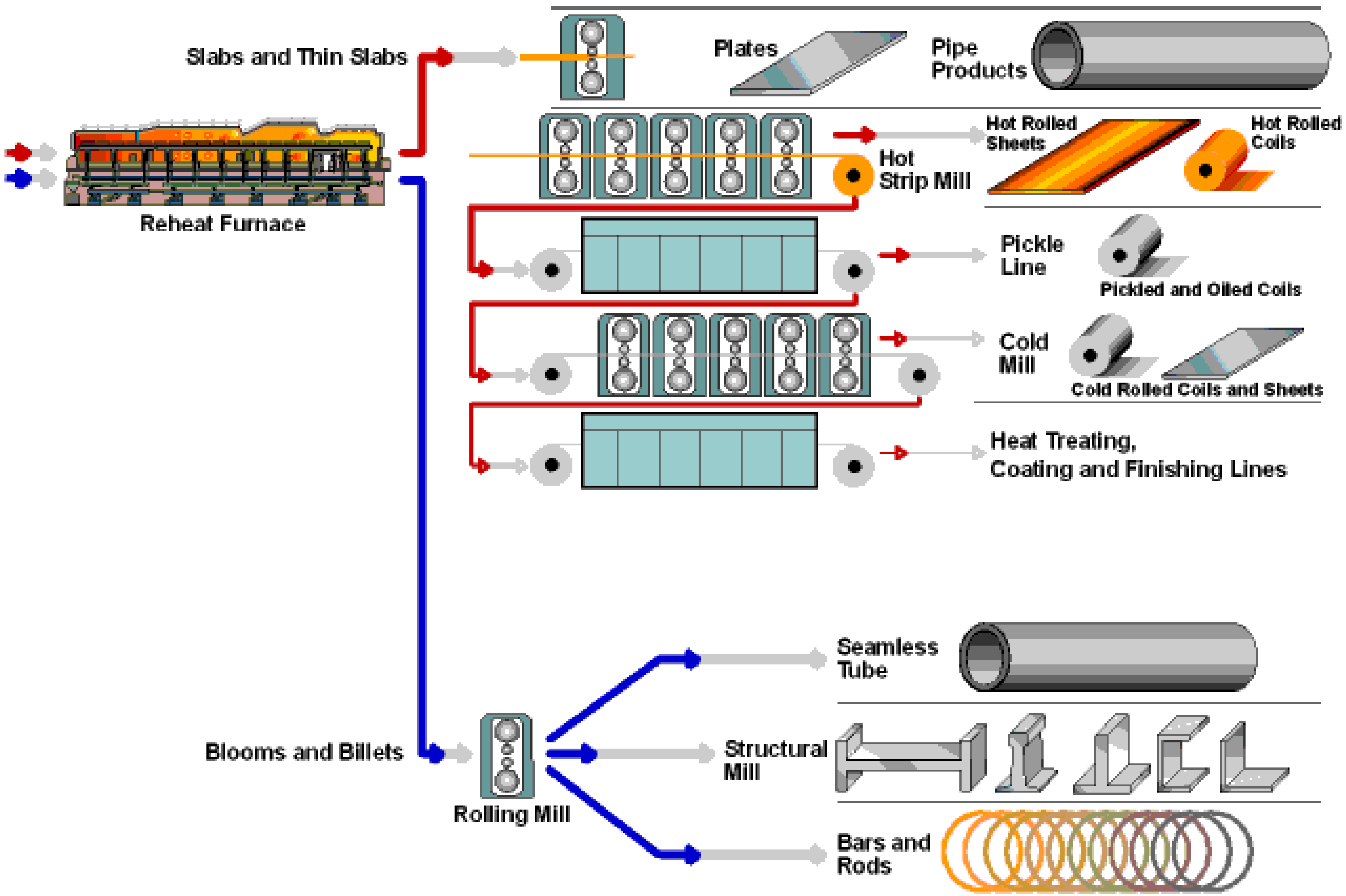

4.6 Solidification during quenching from the melt

Time Temperature Transformation diagram

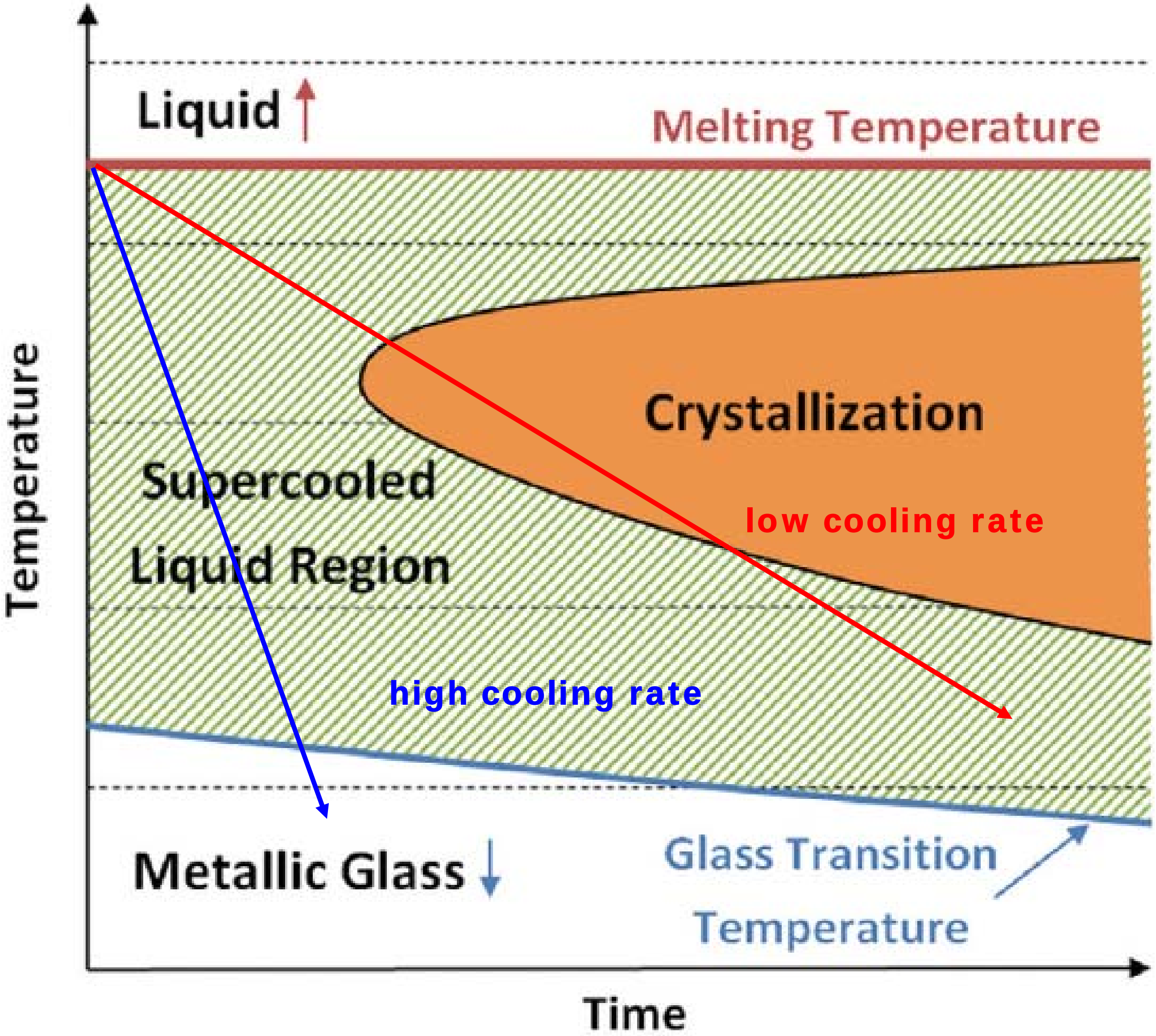

T_g = *fictive temperature*, T_f

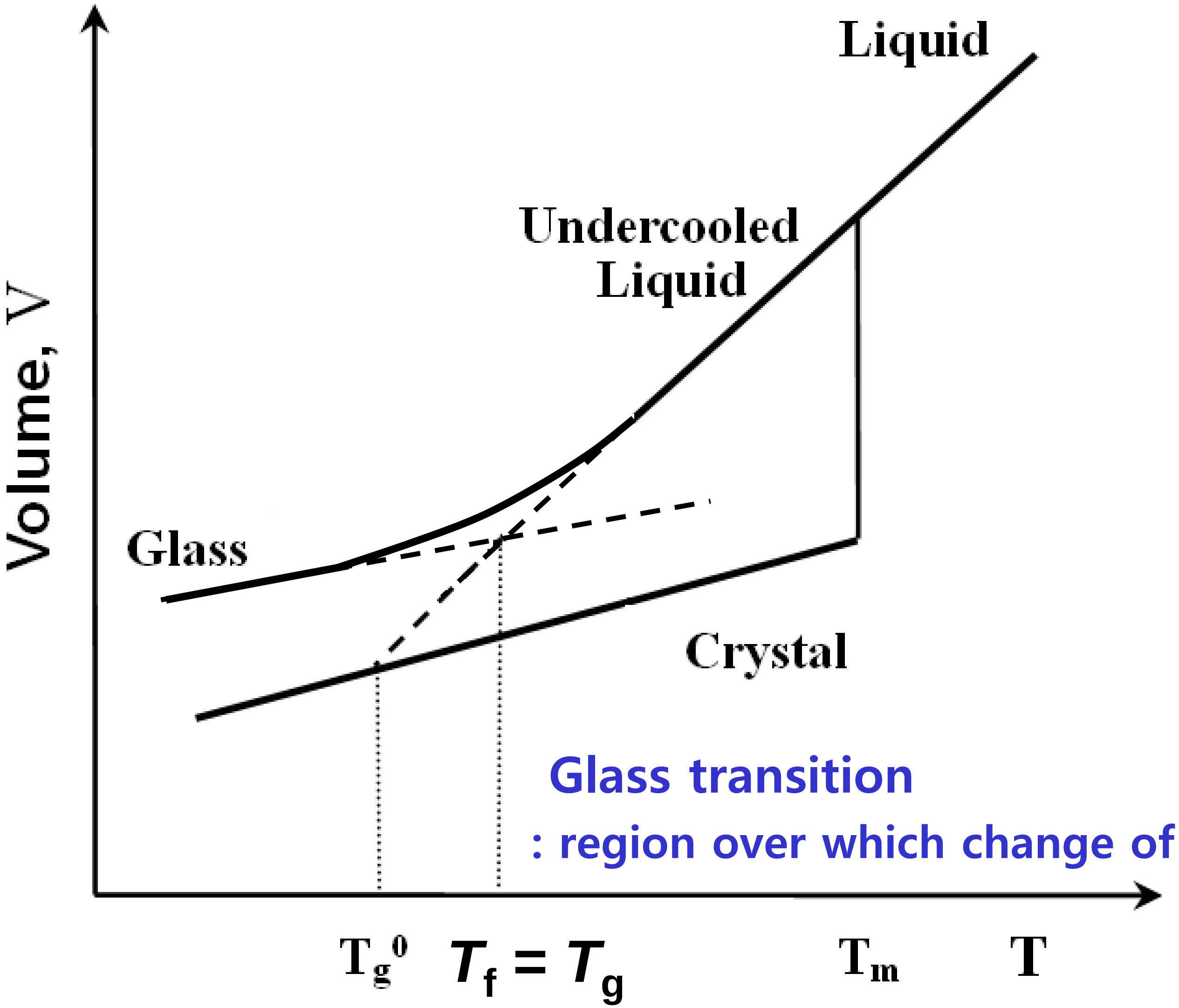

Glass transition

: region over which change of slope occurs

* T_g depends on thermal history.

Kinetic Nature of the Glass Transition

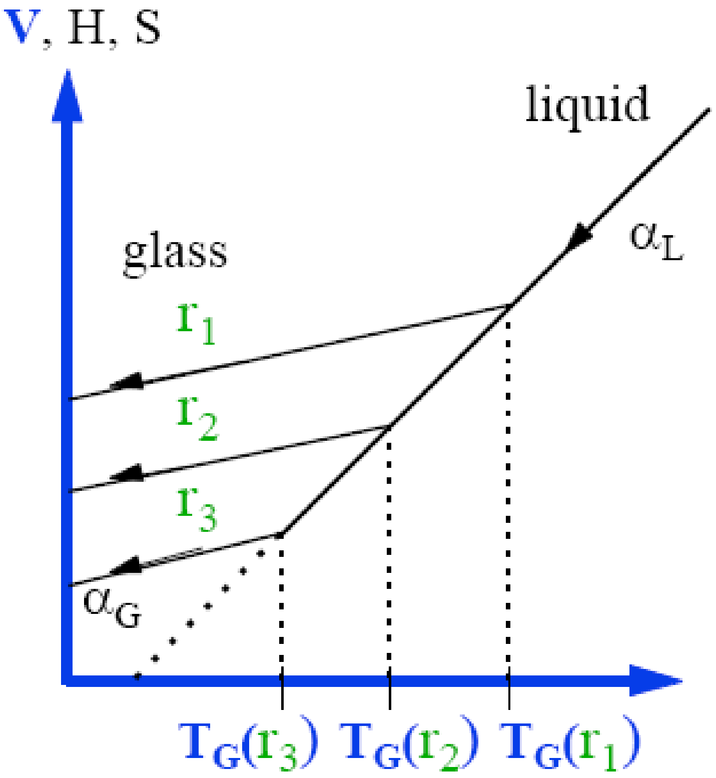

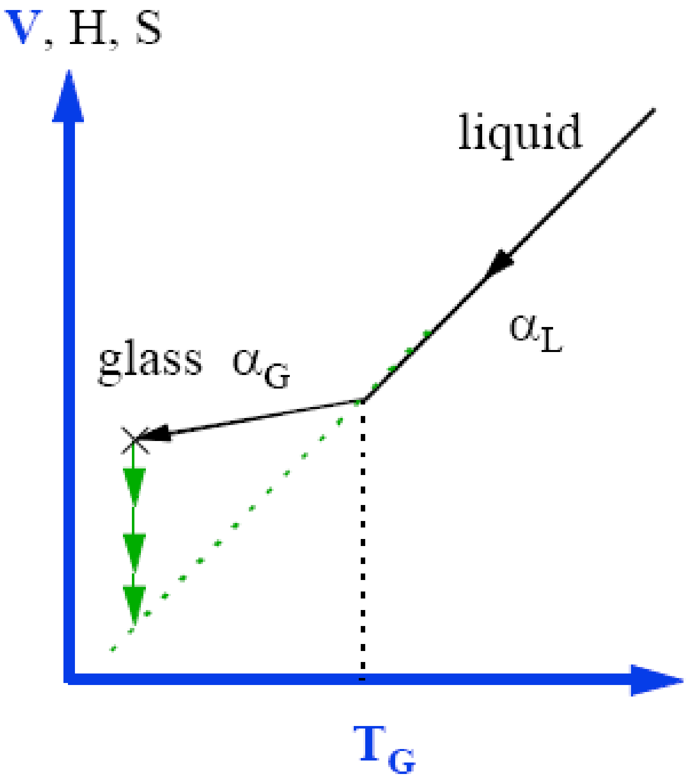

Tg depends on the rate at which the liquid is cooled. $T_G(r_3) < T_G(r_2) < T_G(r_1)$ if $r_3 < r_2 < r_1$

Specific Volume (density) of the glass depends on the time at a given $T < T_g$

Glass formation

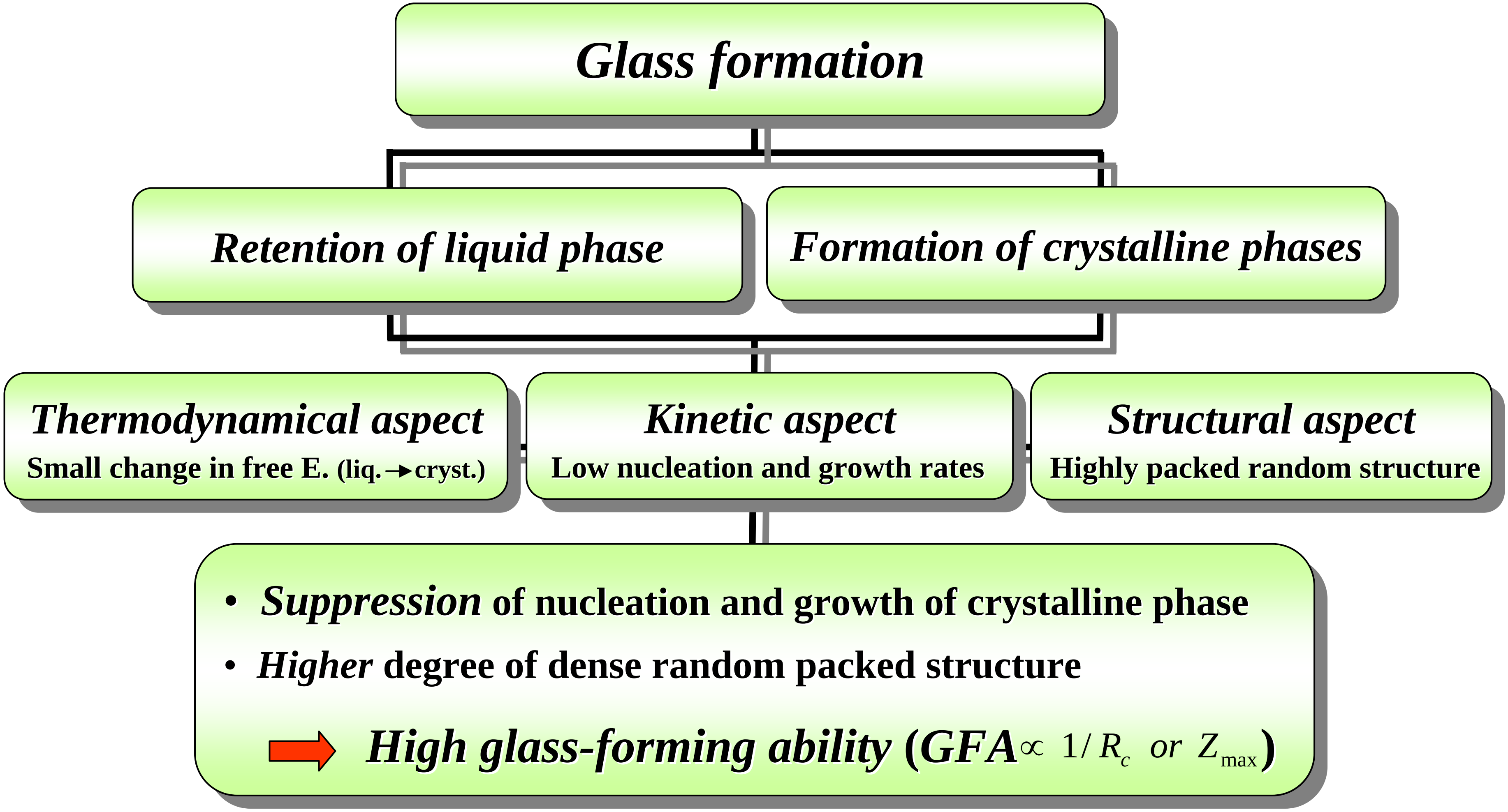

Glass formation

Retention of liquid phase

Formation of crystalline phases

Thermodynamical aspect

Small change in free E. (liq.→cryst.)

Kinetic aspect

Low nucleation and growth rates

Structural aspect

Highly packed random structure

- ***Suppression* of nucleation and growth of crystalline phase**
- ***Higher* degree of dense random packed structure**

➡ ***High glass-forming ability* (*GFA* $\propto 1/R_c$ *or* $Z_{\max}$)**

Glass formation: stabilizing the liquid phase

- **First metallic glass ($Au_{80}Si_{20}$) produced by splat quenching at Caltech by Pol Duwez in 1960.**

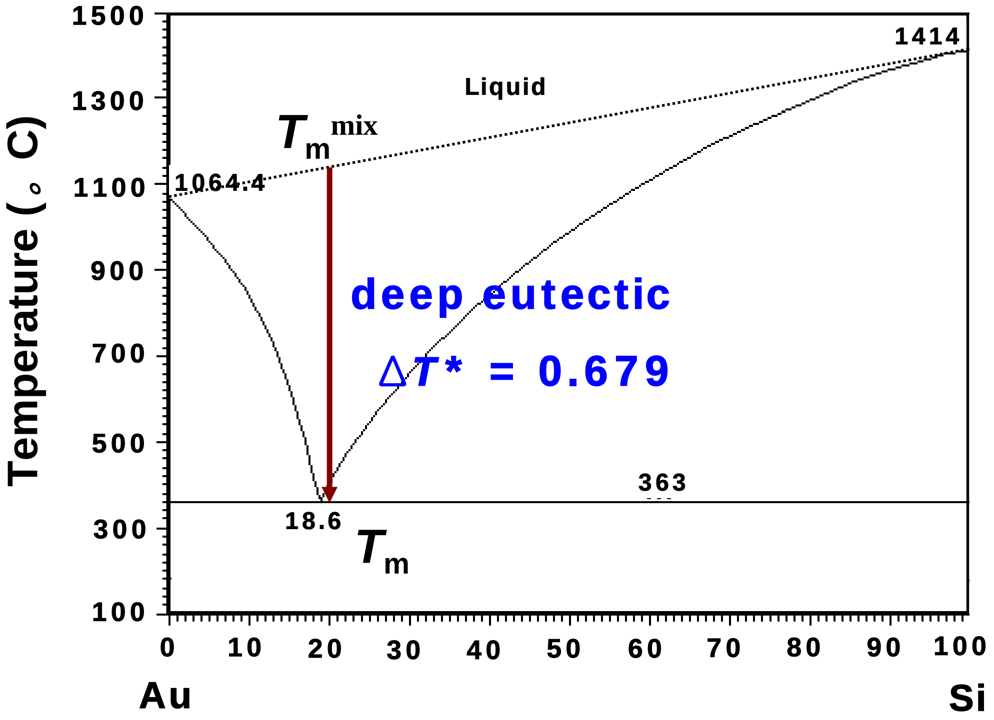

W. Klement, R.H. Willens, P. Duwez, Nature 1960; ***187****: 869.*

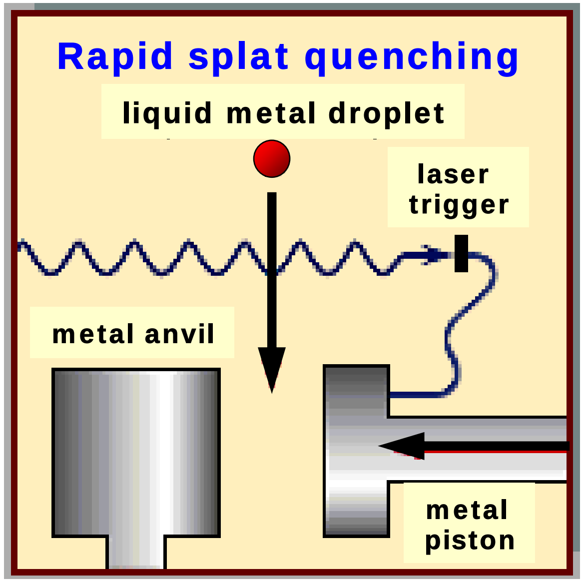

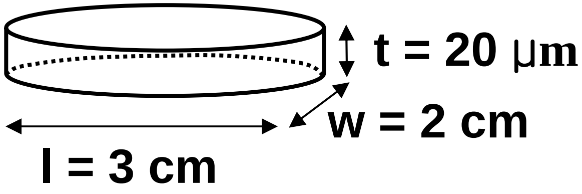

Bulk formation of metallic glass

- **First bulk metallic glass**

$Pd_{77.5}Cu_6Si_{16.5}$ ($T_{rg}=0.64$)

By droplet quenching (CR~800 K/s)

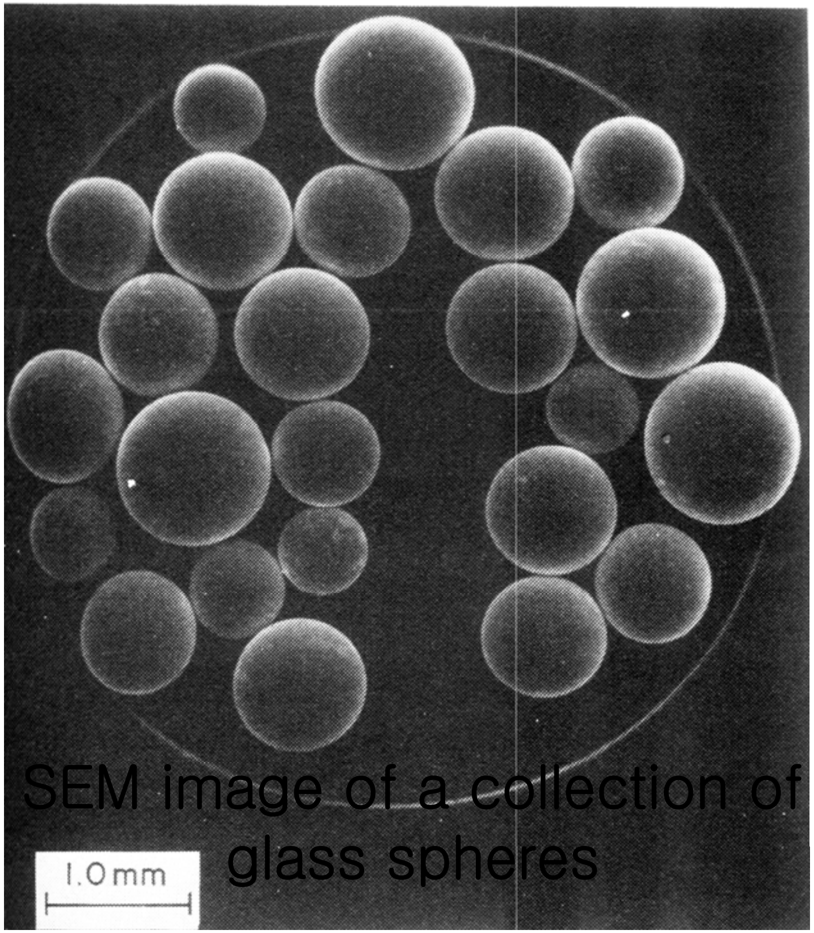

SEM image of a collection of glass spheres

H.S. Chen and D. Turnbull, Acta Metall. 1969; 17: 1021.

Alloy Selection: consideration of T_{rg}

$Pd_{40}Ni_{40}P_{20}$ ($T_{rg}=0.67$)

Suppression of heterogeneous nucleation

- **Largest ingot**

- minimum dimension 1 cm and mass of 4 g
- Critical cooling rate: ~ 1K/sec.

Drehman, Greer, and Turnbull, 1982.

Bulk glass formation in the Pd-Ni-P system

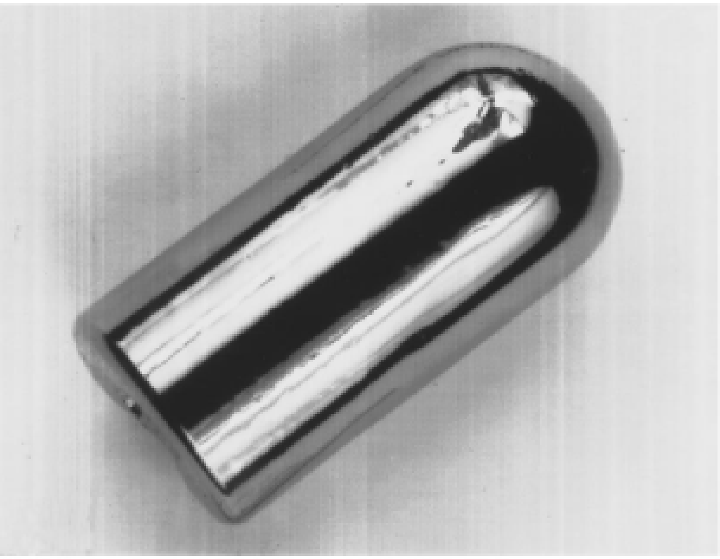

FIG. 1. 300-g ingot of bulk amorphous $Pd_{40}Ni_{40}P_{20}$ rod with 25 mm in diamter prepared by fluxing in B_2O_3 and water quenching.

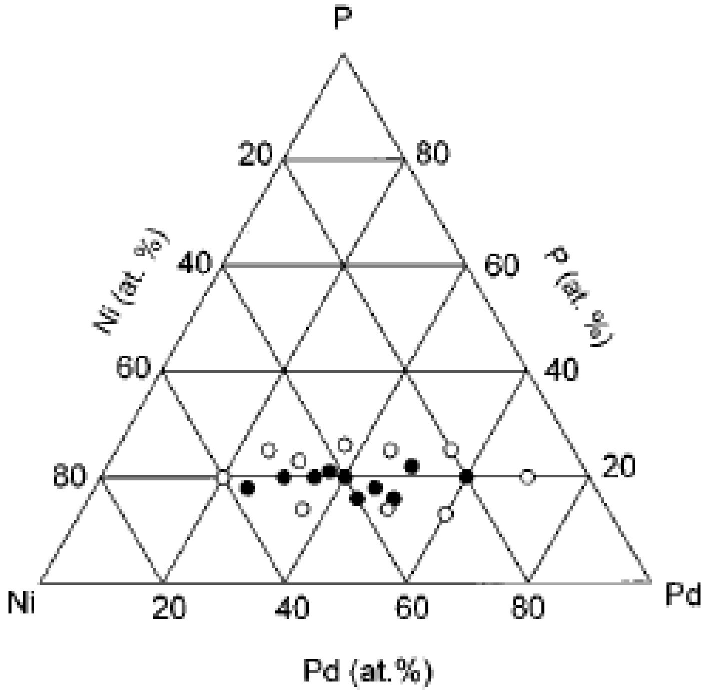

- **Experimental Difference**

1. Arc melting for the ingot : process temperature > 3000 K

2. Water quenching : Improvement of cooling rate

**Y.He, R.B. Schwarz, J.I. Archuleta, Appl. Phys. Lett. 1996; 69: 1861.*

Bulk glass formation in the $Pd_{40}Ni_{10}Cu_{30}P_{20}$ system

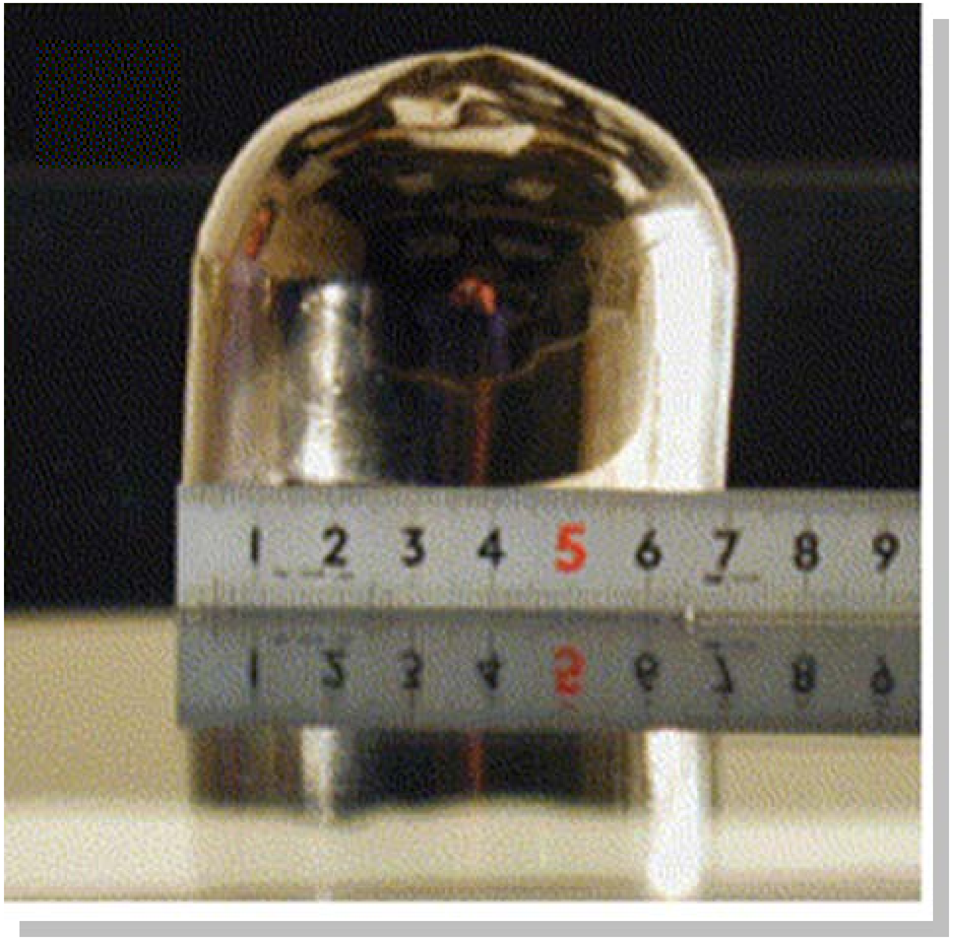

- **Largest ingot**

maximum diameter for glass formation : 72 mm

Critical cooling rate: ~ 0.1K/sec.

How to make bulk metallic glasses

< Casting >

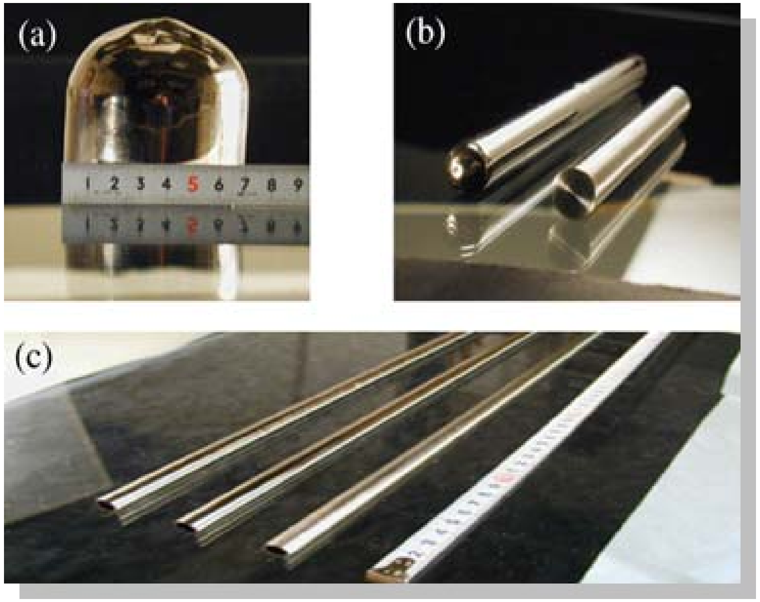

1) Injection casting

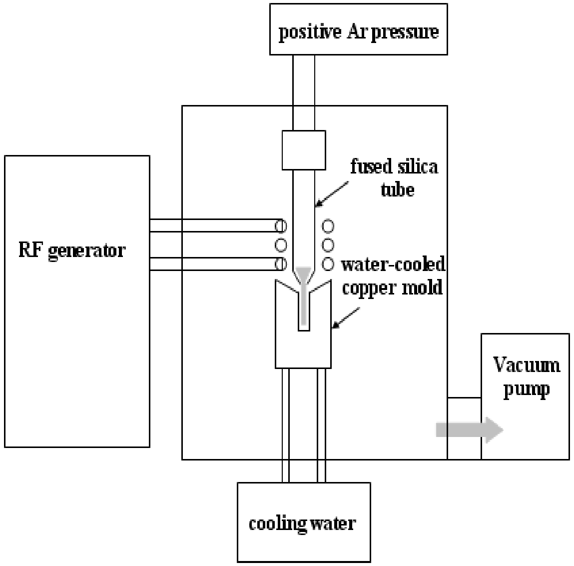

2) Squeeze casting

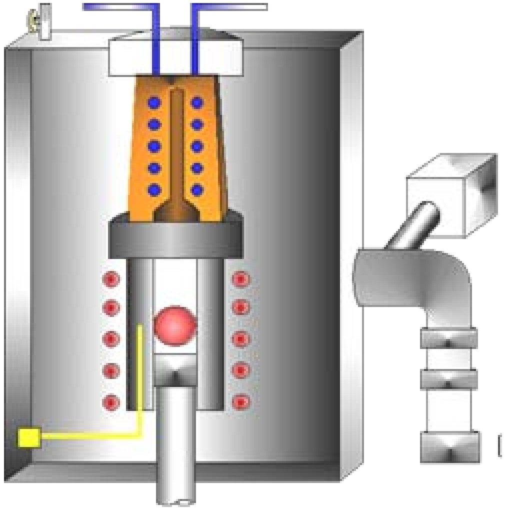

3) Strip casting

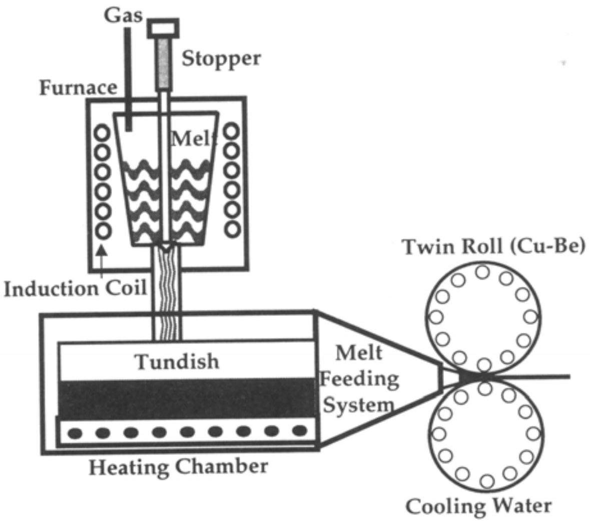

How to make bulk metallic glasses

< Powder Metallurgy>

1) Extrusion

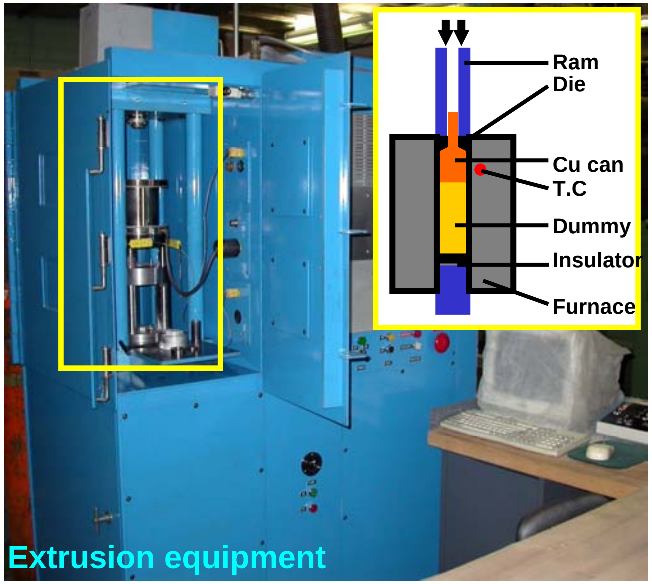

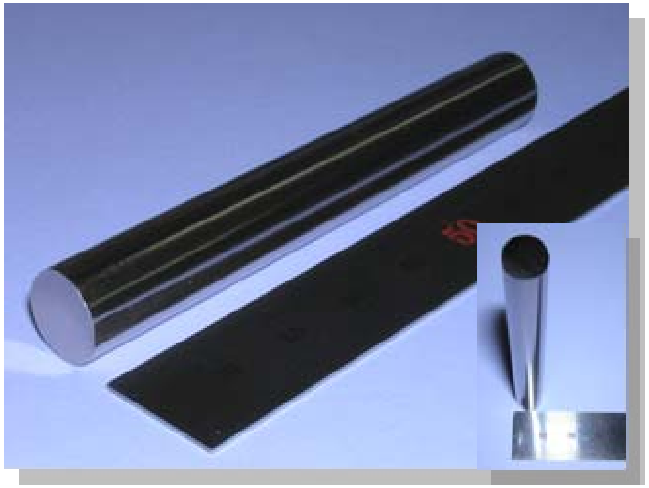

2) Spark Plasma Sintering

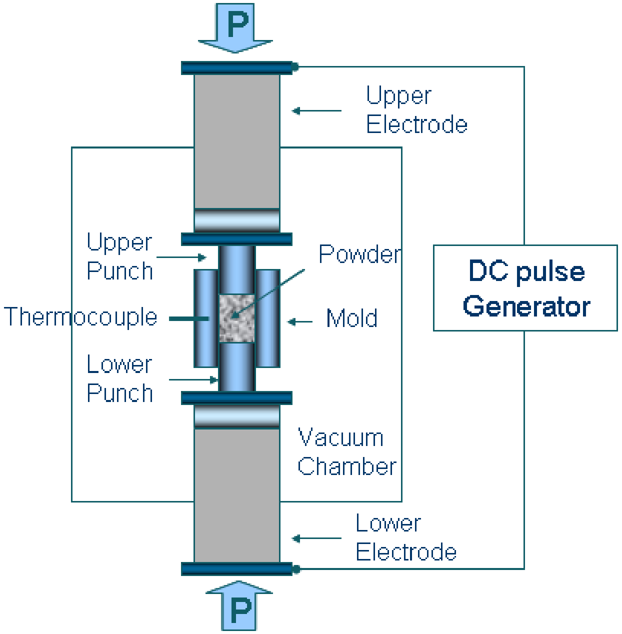

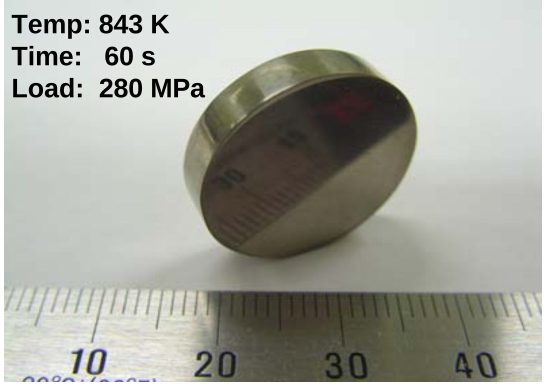

Temp: 843 K
Time: 60 s
Load: 280 MPa

Recent BMGs with critical size ≥ 10 mm

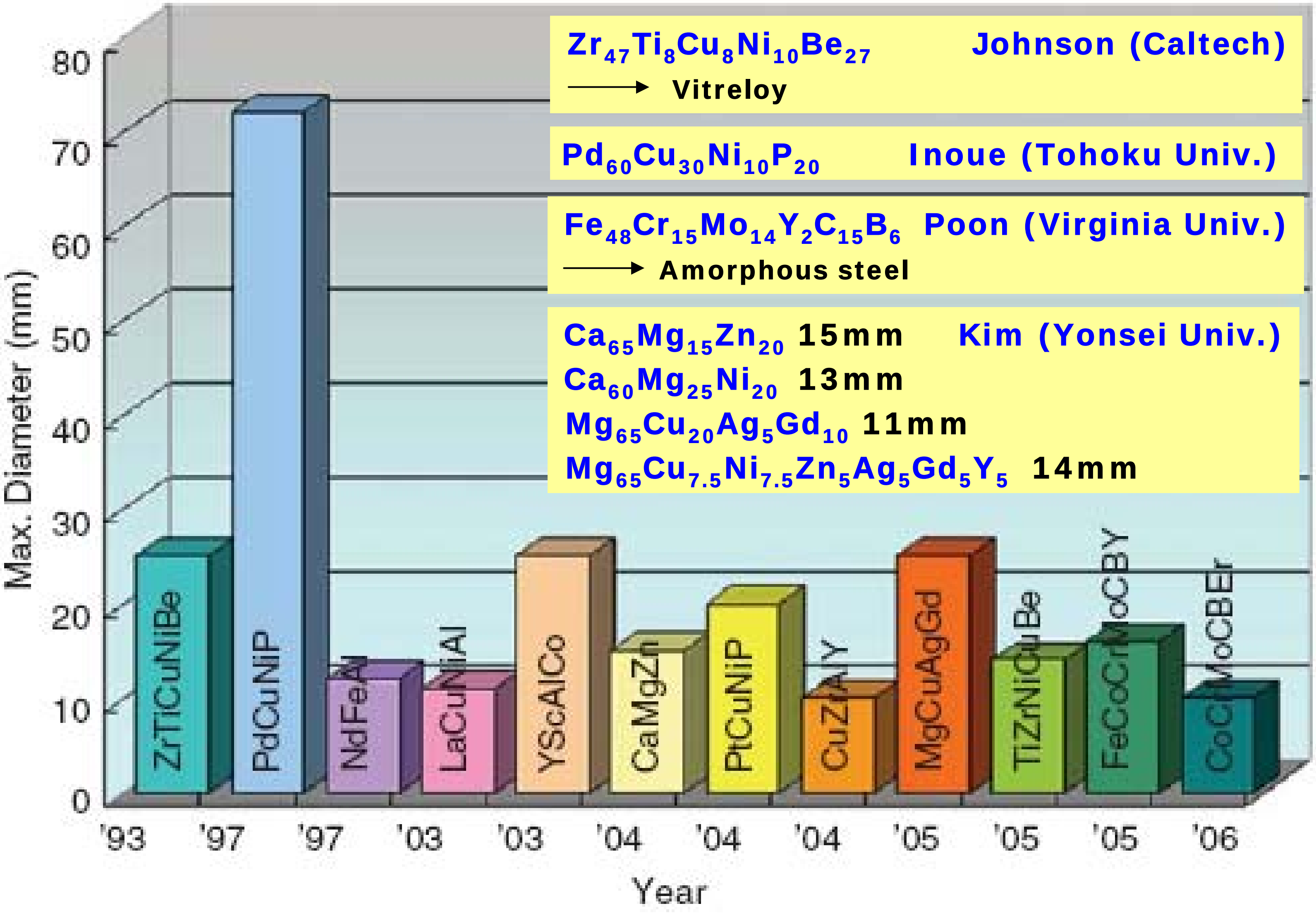

$Zr_{47}Ti_8Cu_8Ni_{10}Be_{27}$ **Johnson (Caltech)**

→ **Vitreloy**

$Pd_{60}Cu_{30}Ni_{10}P_{20}$ **Inoue (Tohoku Univ.)**

$Fe_{48}Cr_{15}Mo_{14}Y_2C_{15}B_6$ **Poon (Virginia Univ.)**

→ **Amorphous steel**

$Ca_{65}Mg_{15}Zn_{20}$ 15mm **Kim (Yonsei Univ.)**
$Ca_{60}Mg_{25}Ni_{20}$ 13mm
$Mg_{65}Cu_{20}Ag_5Gd_{10}$ 11mm
$Mg_{65}Cu_{7.5}Ni_{7.5}Zn_5Ag_5Gd_5Y_5$ 14mm

A.L. Greer, E. Ma, MRS Bulletin, 2007; 32: 612.